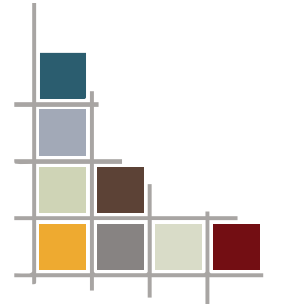


Virtual Patho-Histology at the GINIX 3D X-ray Microscope

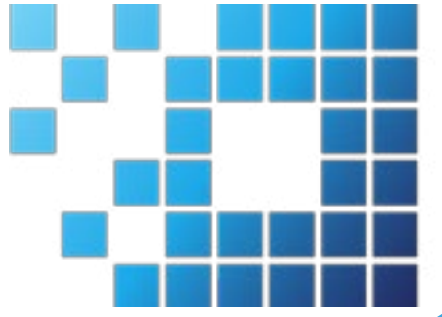
Markus Osterhoff
Institut für Röntgenphysik,
Uni Göttingen



SFB
755



Verbundforschung
/ ErUM

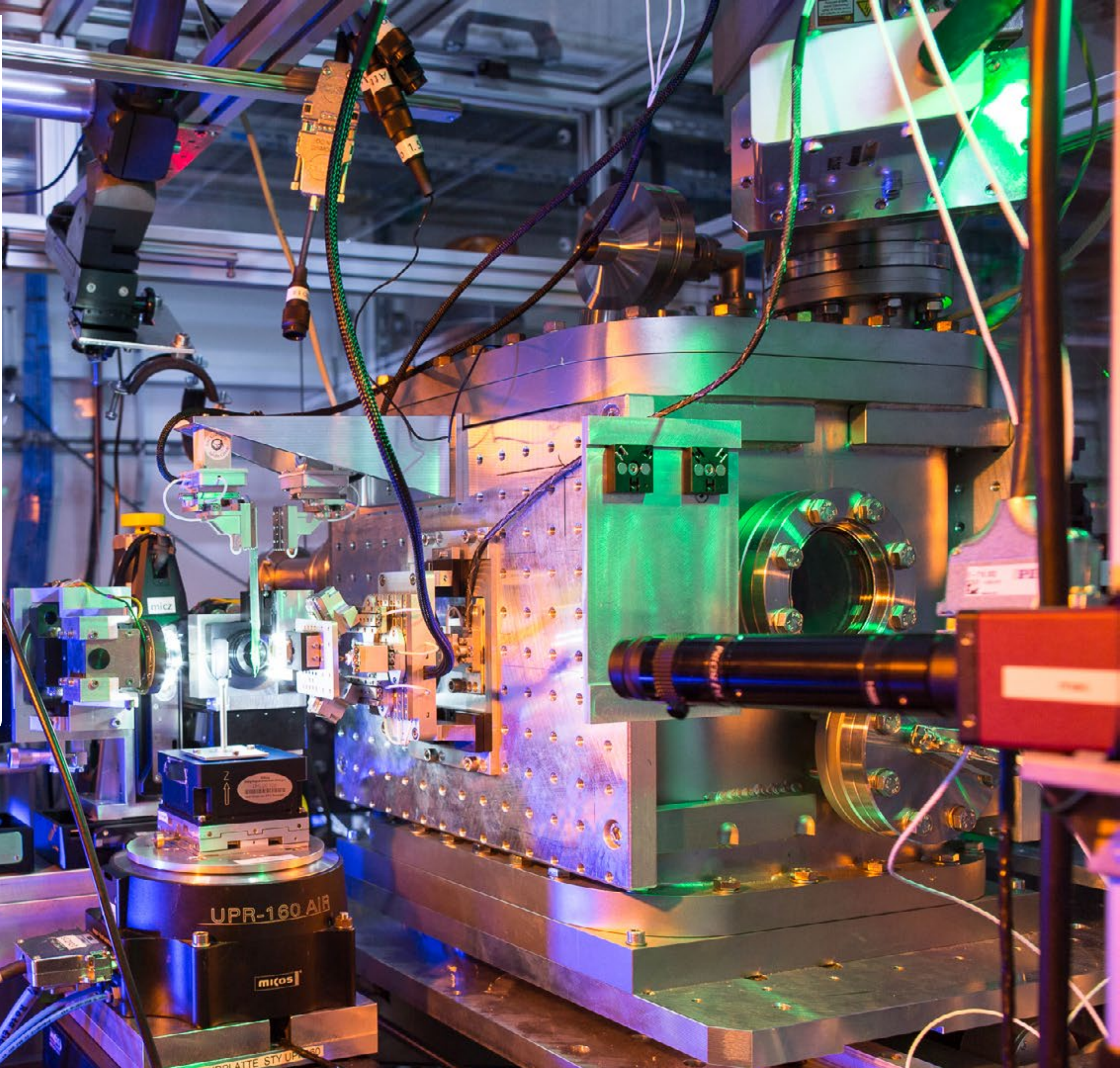


CRC 1456
MATHEMATICS
OF EXPERIMENT

CIDAS
Campus-Institut Data Science



bmb+f
Großgeräte
der physikalischen
Grundlagenforschung

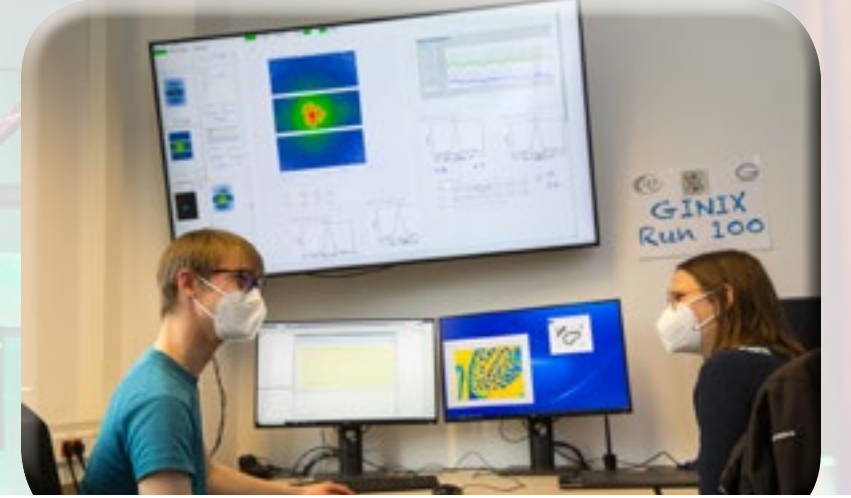
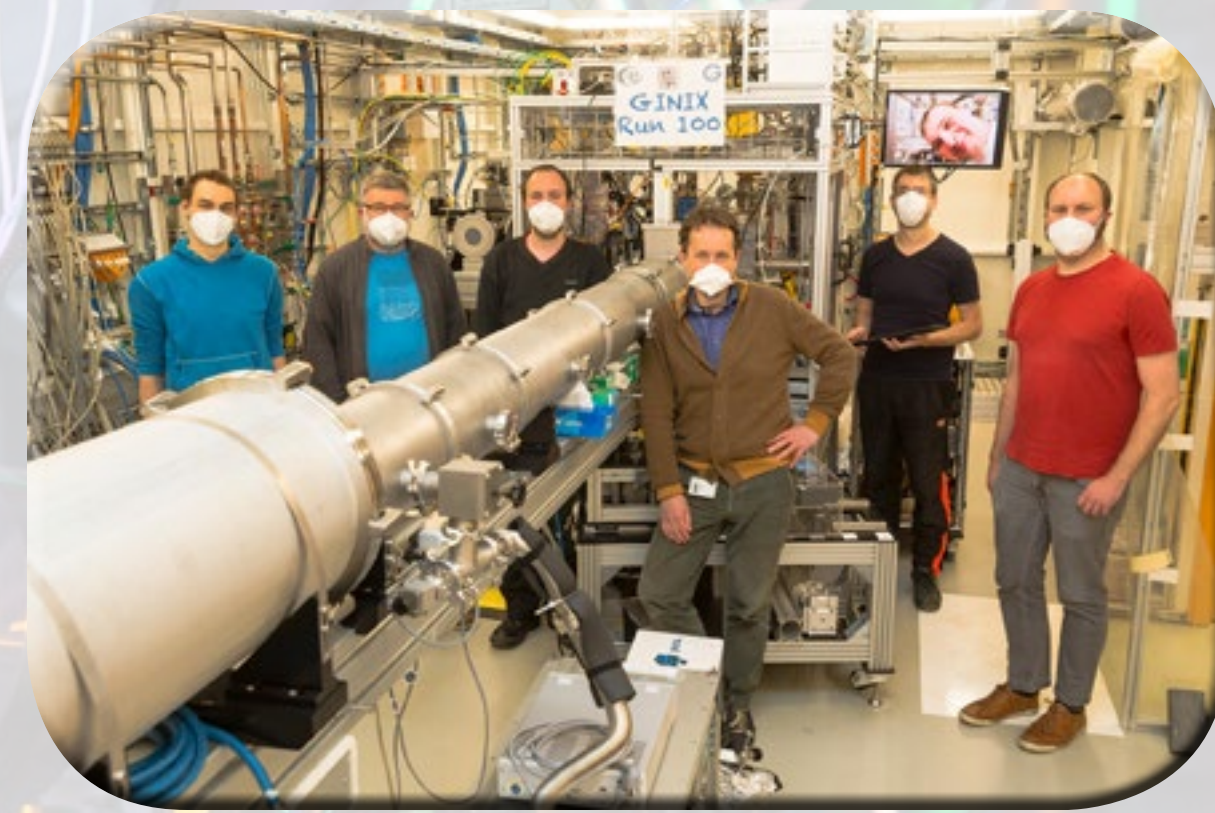
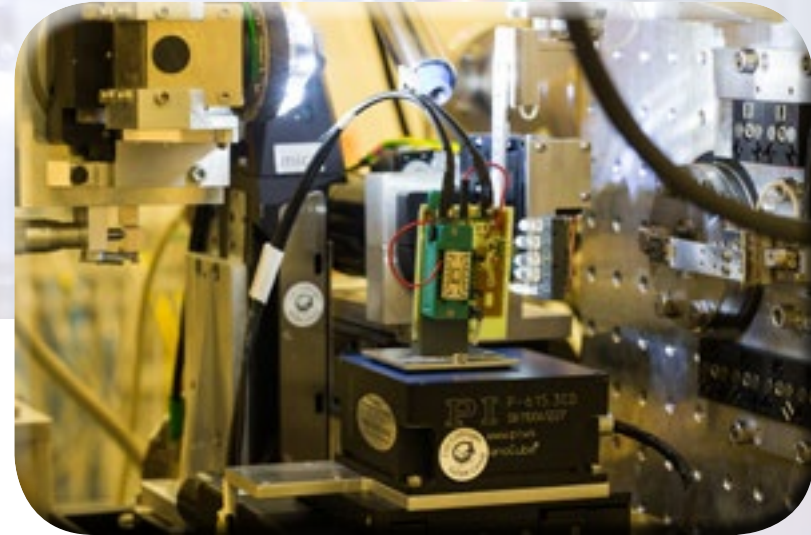


Virtual Patho-Histology at the GINIX 3D X-ray Micro

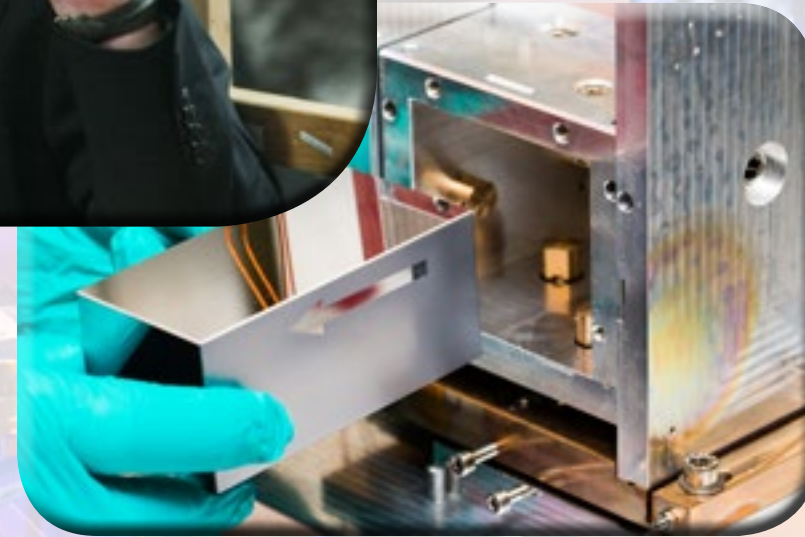
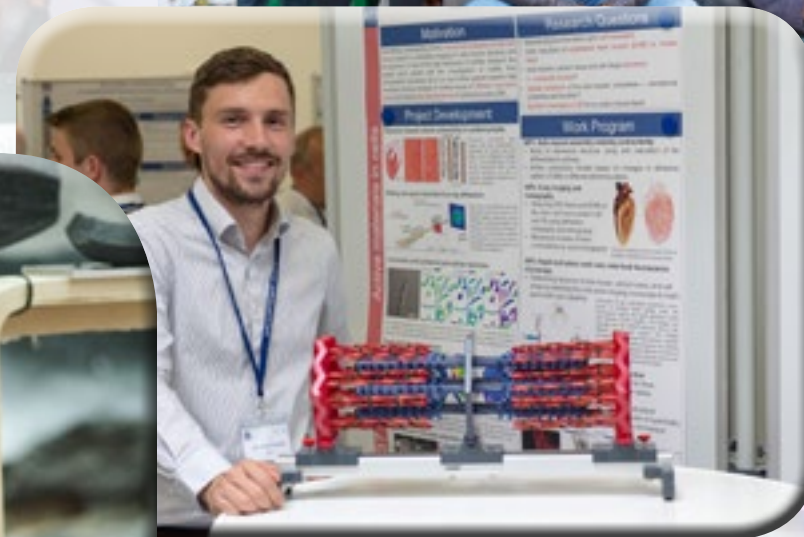
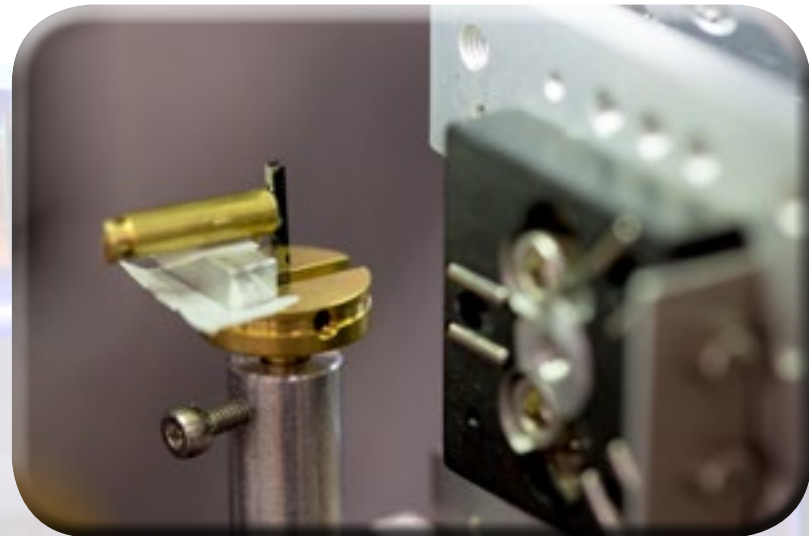
Markus Osterhoff
Institut für Röntgenphysik,
U



BMBF: 05KS7MG, 05K10MGA
05K13MG4, 05K16MG2 (STED),
05K16MGA (Nanosolar),
05K16MGB, 05K19MG2 (Neurotomo)
DFG: SFB 755



Sebastian Kalbfleisch, Bastian Hartmann
Peter Luley, Jan Goeman,
Mike Kanbach + workshops;
Matthias Bartels, Martin Krenkel,
Marten Bernhardt, Mareike Töpferwien,
Jakob Soltau, Marina Eckermann,
Jasper Frohn, ...



<p>run100 Instrument: GINIX Group: Salditt 2021-04-09 – 2021-04-26</p>	<p>run11 Instrument: GINIX Group: extern 2020-10-10 – 2020-10-14</p>	<p>run12 Instrument: GINIX Group: Salditt 2020-10-05 – 2020-10-10</p>	<p>run13 Instrument: GINIX Group: extern 2020-09-26 – 2020-10-05</p>	<p>run16 Instrument: GINIX Group: Salditt 2020-09-19 – 2020-09-28</p>	<p>run17 Instrument: GINIX Group: Salditt 2020-05-06 – 2020-05-13</p>	<p>run19 Instrument: GINIX Group: Salditt 2020-04-23 – 2020-05-06</p>	<p>run23 Instrument: GINIX Group: extern 2019-09-28 – 2019-10-01</p>	<p>run24 Instrument: GINIX Group: Salditt 2019-09-23 – 2019-09-28</p>	<p>run27 Instrument: GINIX Group: extern 2019-09-18 – 2019-09-23</p>	<p>run30 Instrument: GINIX Group: extern 2019-09-14 – 2019-09-18</p>	<p>run31 Instrument: GINIX Group: Salditt 2019-09-04 – 2019-09-14</p>	<p>run32 Instrument: GINIX Group: Salditt 2019-07-03</p>	<p>run36 Instrument: GINIX Group: Salditt 2019-06-22 – 2019-06-26</p>	<p>run38 Instrument: GINIX Group: Küster 2019-06-17 – 2019-06-22</p>	<p>run39 Instrument: GINIX Group: Salditt 2019-06-15 – 2019-06-17</p>	
<p>run42 Instrument: GINIX Group: extern 2019-04-14 – 2019-04-17</p>	<p>run43 Instrument: GINIX Group: extern 2019-04-09 – 2019-04-14</p>	<p>run44 Instrument: GINIX Group: Salditt 2019-04-04 – 2019-04-09</p>	<p>run49 Instrument: GINIX Group: extern 2018-11-07 – 2018-11-08</p>	<p>run50 Instrument: GINIX Group: Salditt 2018-10-27 – 2018-11-07</p>	<p>run53 Instrument: GINIX Group: IRP 2018-05-30 – 2018-06-04</p>	<p>run54 Instrument: GINIX Group: extern 2018-05-28 – 2018-05-30</p>	<p>run56 Instrument: GINIX Group: extern 2018-05-23 – 2018-05-28</p>	<p>run57 Instrument: GINIX Group: Salditt 2018-05-17 – 2018-05-23</p>	<p>run59 Instrument: GINIX Group: Küster 2017-11-29 – 2017-12-06</p>	<p>run60 Instrument: GINIX Group: extern 2017-11-26 – 2017-11-29</p>	<p>run61 Instrument: GINIX Group: extern 2017-11-22 – 2017-11-26</p>	<p>run68 Instrument: GINIX Group: extern 2017-11-18 – 2017-11-22</p>	<p>run69 Instrument: GINIX Group: Salditt 2017-11-08 – 2017-11-18</p>			
<p>run66 Instrument: GINIX Group: Salditt 2017-09-20 – 2017-09-25</p>	<p>run65 Instrument: GINIX Group: Salditt 2017-09-17 – 2017-09-20</p>	<p>run67 Instrument: GINIX Group: Salditt 2017-06-14 – 2017-06-17</p>	<p>run63 Instrument: GINIX Group: extern 2017-06-02 – 2017-06-07</p>	<p>run62 Instrument: GINIX Group: Salditt 2017-05-26 – 2017-06-02</p>	<p>run64 Instrument: GINIX Group: IRP 2017-05-19 – 2017-05-26</p>	<p>run69 Instrument: GINIX Group: Küster 2016-11-28 – 2016-12-02</p>	<p>run70 Instrument: GINIX Group: Salditt 2016-11-17 – 2016-11-28</p>	<p>run71 Instrument: GINIX Group: Salditt 2016-06-13 – 2016-06-15</p>	<p>run72 Instrument: GINIX Group: Salditt 2016-06-08 – 2016-06-12</p>	<p>run73 Instrument: GINIX Group: extern 2016-06-05 – 2016-06-08</p>	<p>run74 Instrument: GINIX Group: extern 2016-06-01 – 2016-06-05</p>	<p>run51 Instrument: GINIX Group: Salditt 2016-05-25 – 2016-06-01</p>	<p>run50 Instrument: GINIX Group: Salditt 2016-05-18 – 2016-05-25</p>			
<p>run77 Instrument: GINIX Group: Salditt 2015-10-07 – 2015-10-13</p>	<p>run78 Instrument: GINIX Group: Salditt 2015-09-30 – 2015-10-05</p>	<p>run79 Instrument: GINIX Group: extern 2015-09-23 – 2015-09-30</p>	<p>run96 Instrument: GINIX Group: extern 2015-09-19 – 2015-09-23</p>	<p>run95 Instrun. Group: e 2015-09-1</p>	<p>run94 Instrument: GINIX Group: Salditt 2015-09-04 – 2015-09-10</p>	<p>run93 Instrument: GINIX Group: Salditt 2015-05-06 – 2015-05-13</p>	<p>run92 Instrument: GINIX Group: Küster 2015-05-01 – 2015-05-06</p>	<p>run90 Instrument: GINIX Group: Salditt 2015-04-17 – 2015-05-01</p>	<p>run89 Instrument: GINIX Group: Salditt 2014-01-03 – 2014-01-08</p>	<p>run88 Instrument: GINIX Group: Salditt 2013-12-11 – 2013-12-19</p>	<p>run87 Instrument: GINIX Group: Salditt 2013-12-05 – 2013-12-11</p>	<p>run86 Instrument: GINIX Group: Salditt 2013-11-13 – 2013-11-18</p>	<p>run85 Instrument: GINIX Group: Salditt 2013-09-25 – 2013-10-02</p>	<p>run84 Instrument: GINIX Group: Salditt 2013-09-23 – 2013-09-25</p>	<p>run83 Instrument: GINIX Group: Salditt 2013-08-28 – 2013-09-20</p>	
<p>run82 Instrument: GINIX Group: extern 2013-06-27 – 2013-07-01</p>	<p>run81 Instrument: GINIX Group: Salditt 2013-06-21 – 2013-06-27</p>	<p>run80 Instrument: GINIX Group: extern 2013-05-04 – 2013-05-08</p>	<p>run75 Instrument: GINIX Group: Salditt 2013-04-28 – 2013-05-03</p>	<p>run76 Instrument: GINIX Group: extern 2013-04-24 – 2013-04-28</p>	<p>run74 Instrument: GINIX Group: extern 2013-04-18 – 2013-04-24</p>	<p>run73 Instrument: GINIX Group: Salditt 2013-04-02 – 2013-04-05</p>	<p>run72 Instrument: GINIX Group: Küster 2013-03-25 – 2013-03-30</p>	<p>run71 Instrument: GINIX Group: extern 2013-03-30 – 2013-03-30</p>	<p>run70 Instrument: GINIX Group: Salditt 2013-03-16 – 2013-03-25</p>	<p>run69 Instrument: GINIX Group: Salditt 2013-03-11 – 2013-03-16</p>	<p>run68 Instrument: GINIX Group: Salditt 2013-03-07 – 2013-03-11</p>	<p>run67 Instrument: GINIX Group: Salditt 2012-10-17 – 2012-10-22</p>	<p>run66 Instrument: GINIX Group: extern 2012-10-15 – 2012-10-17</p>	<p>run65 Instrument: GINIX Group: extern 2012-10-11 – 2012-10-15</p>	<p>run64 Instrument: GINIX Group: Salditt 2012-10-05 – 2012-10-10</p>	<p>run63 Instrument: GINIX Group: Salditt 2012-10-01 – 2012-10-05</p>
<p>run55 Instrument: GINIX Group: Salditt 2012-10-01 – 2012-10-05</p>	<p>run54 Instrument: GINIX Group: Salditt 2012-10-01 – 2012-10-05</p>	<p>run53 Instrument: GINIX Group: Salditt 2012-10-01 – 2012-10-05</p>	<p>run52 Instrument: GINIX Group: Salditt 2012-10-01 – 2012-10-05</p>	<p>run51 Instrument: GINIX Group: Salditt 2012-10-01 – 2012-10-05</p>	<p>run50 Instrument: GINIX Group: Salditt 2012-10-01 – 2012-10-05</p>	<p>run49 Instrument: GINIX Group: Salditt 2012-10-01 – 2012-10-05</p>	<p>run48 Instrument: GINIX Group: Salditt 2012-10-01 – 2012-10-05</p>	<p>run47 Instrument: GINIX Group: Salditt 2012-10-01 – 2012-10-05</p>	<p>run46 Instrument: GINIX Group: Salditt 2012-10-01 – 2012-10-05</p>	<p>run45 Instrument: GINIX Group: Salditt 2012-10-01 – 2012-10-05</p>	<p>run44 Instrument: GINIX Group: Salditt 2012-10-01 – 2012-10-05</p>	<p>run43 Instrument: GINIX Group: Salditt 2012-10-01 – 2012-10-05</p>	<p>run42 Instrument: GINIX Group: Salditt 2012-10-01 – 2012-10-05</p>	<p>run41 Instrument: GINIX Group: Salditt 2012-10-01 – 2012-10-05</p>	<p>run40 Instrument: GINIX Group: Salditt 2012-10-01 – 2012-10-05</p>	

April 2021: Run 100

Virtual Patho-Histology at the GINIX 3D X-ray Microscope

Markus Osterhoff
Institut für Röntgenphysik,
Uni Göttingen

Introduction

GINIX setup

Holo-Tomo

Methods & Algorithms & AI

Technical Progress, Scientific Results

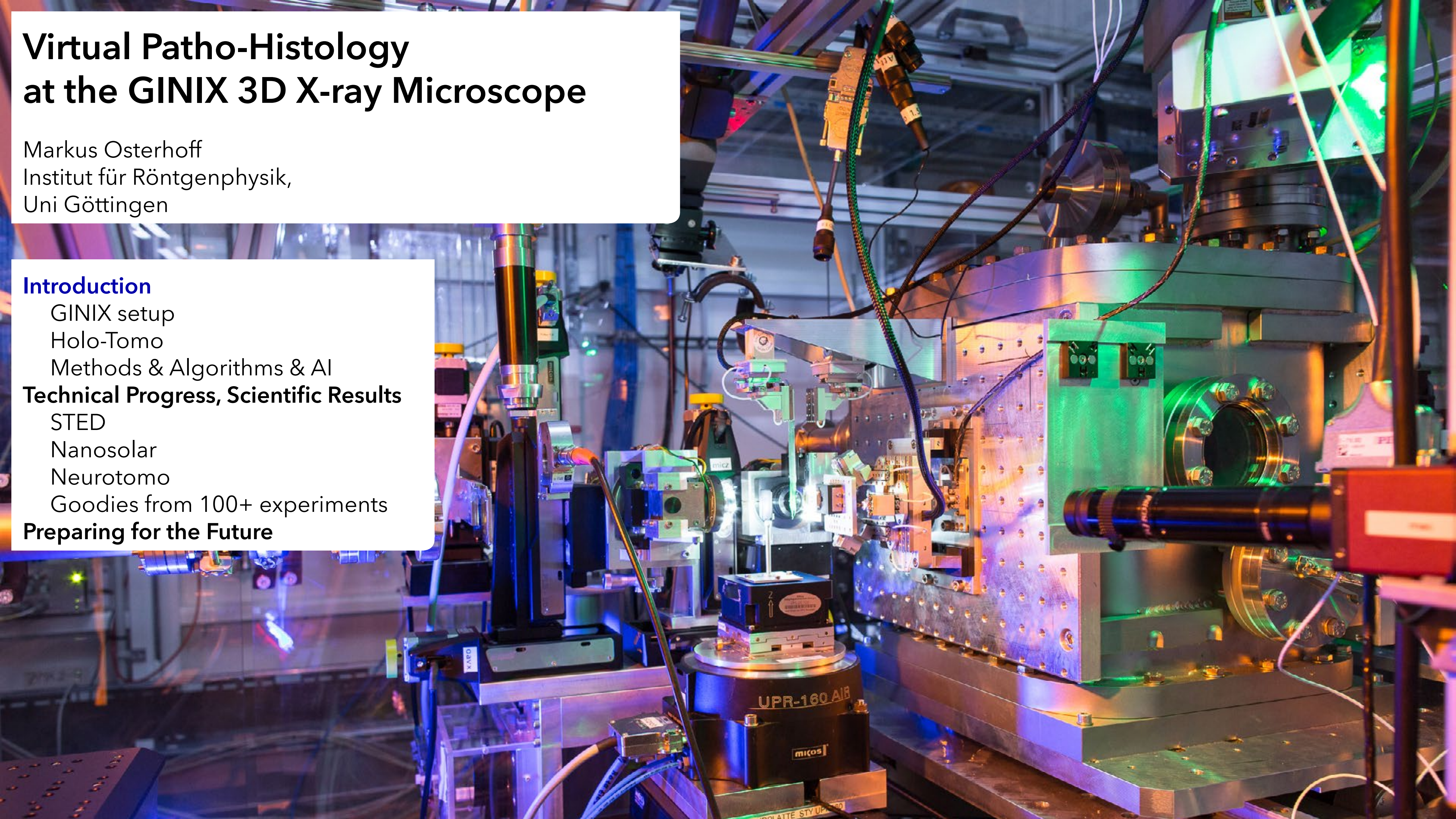
STED

Nanosolar

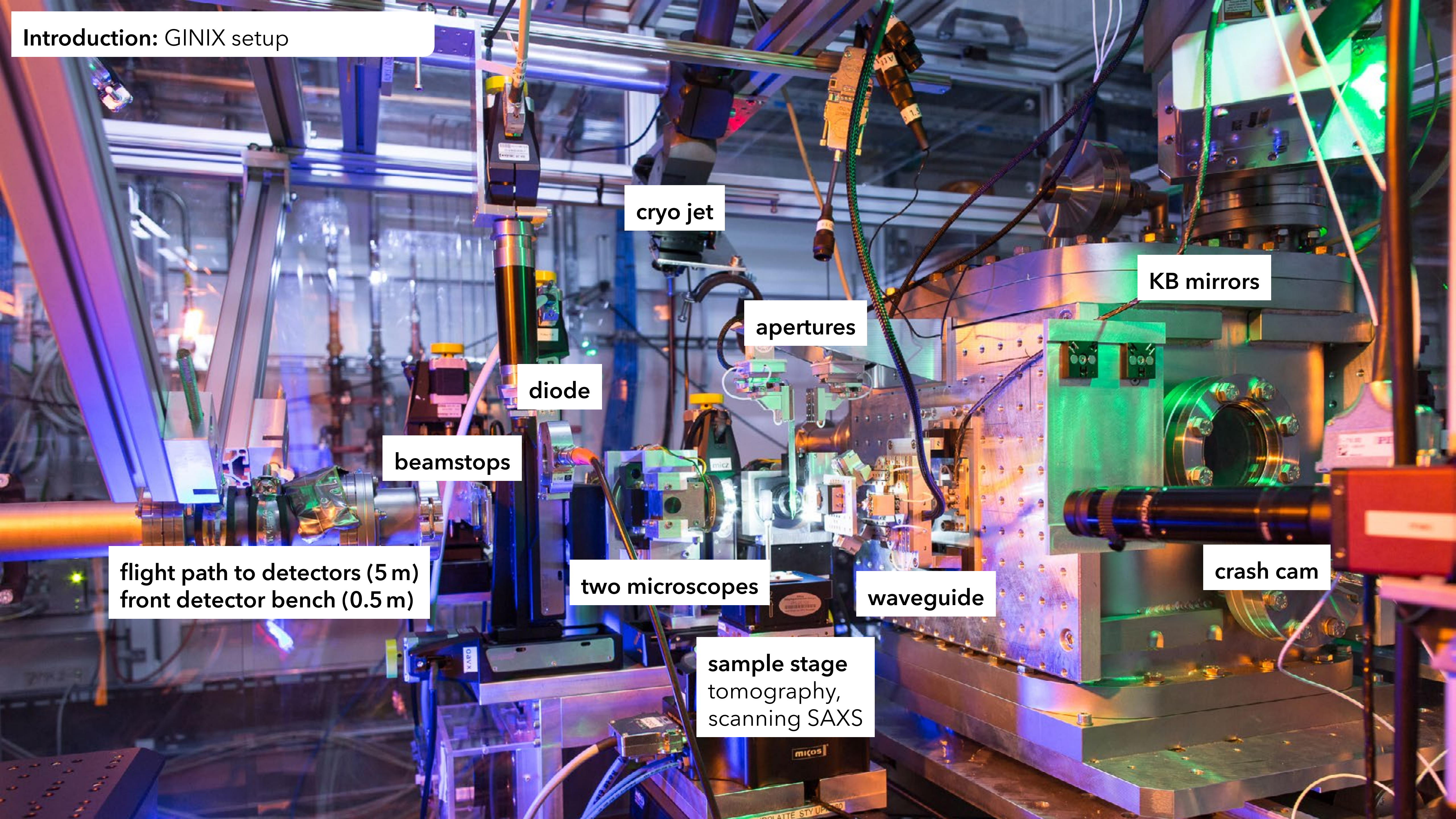
Neurotomo

Goodies from 100+ experiments

Preparing for the Future



Introduction: GINIX setup



cryo jet

KB mirrors

apertures

diode

beamstops

flight path to detectors (5 m)
front detector bench (0.5 m)

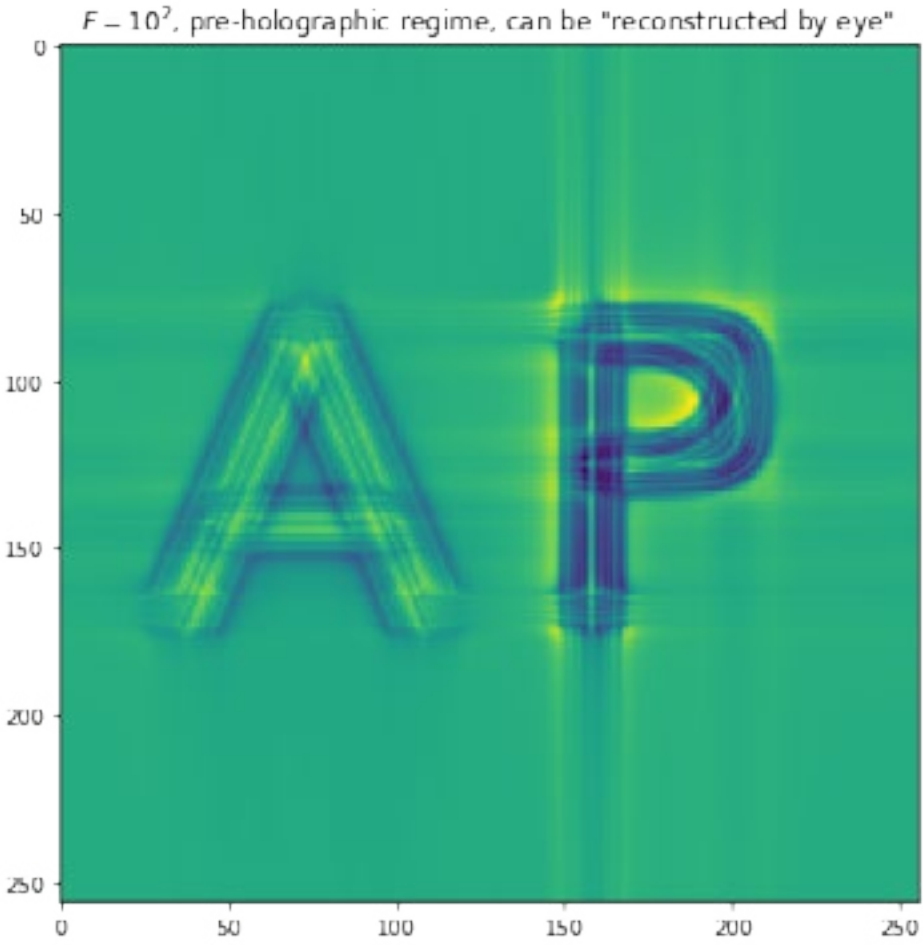
two microscopes

waveguide

crash cam

sample stage
tomography,
scanning SAXS

Introduction: holo-tomo - nano SAXS



Holo-Tomography

Full-field imaging technique

quantitative contrast

- ▶ electron density
- ▶ projected along optical axis
- ▶ phase retrieval / inversion

cone-beam

- ▶ adjustable field of view
- ▶ zooming capability

holo-tomography

- ▶ combined with rotation axis
- ▶ 3D electron density

Scanning nano-SAXS

Raster-scanning technique

periodic structures

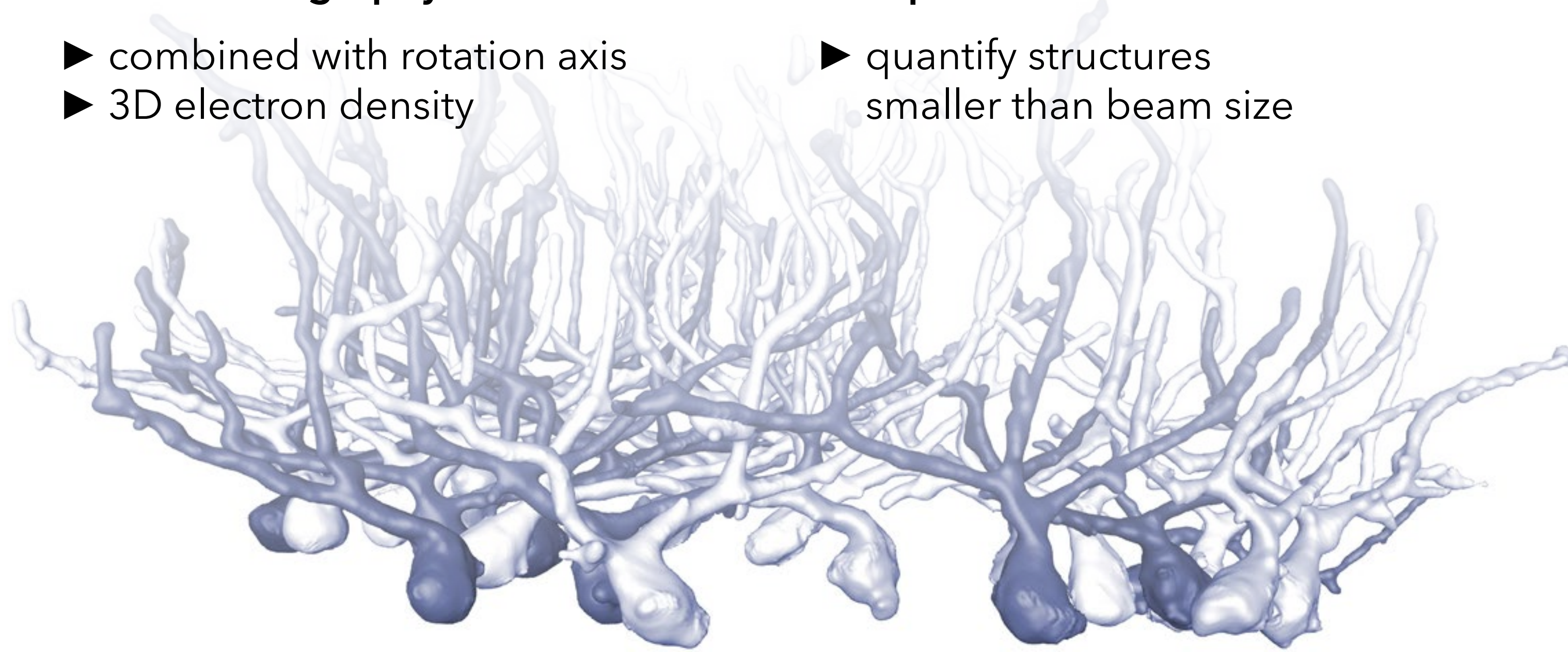
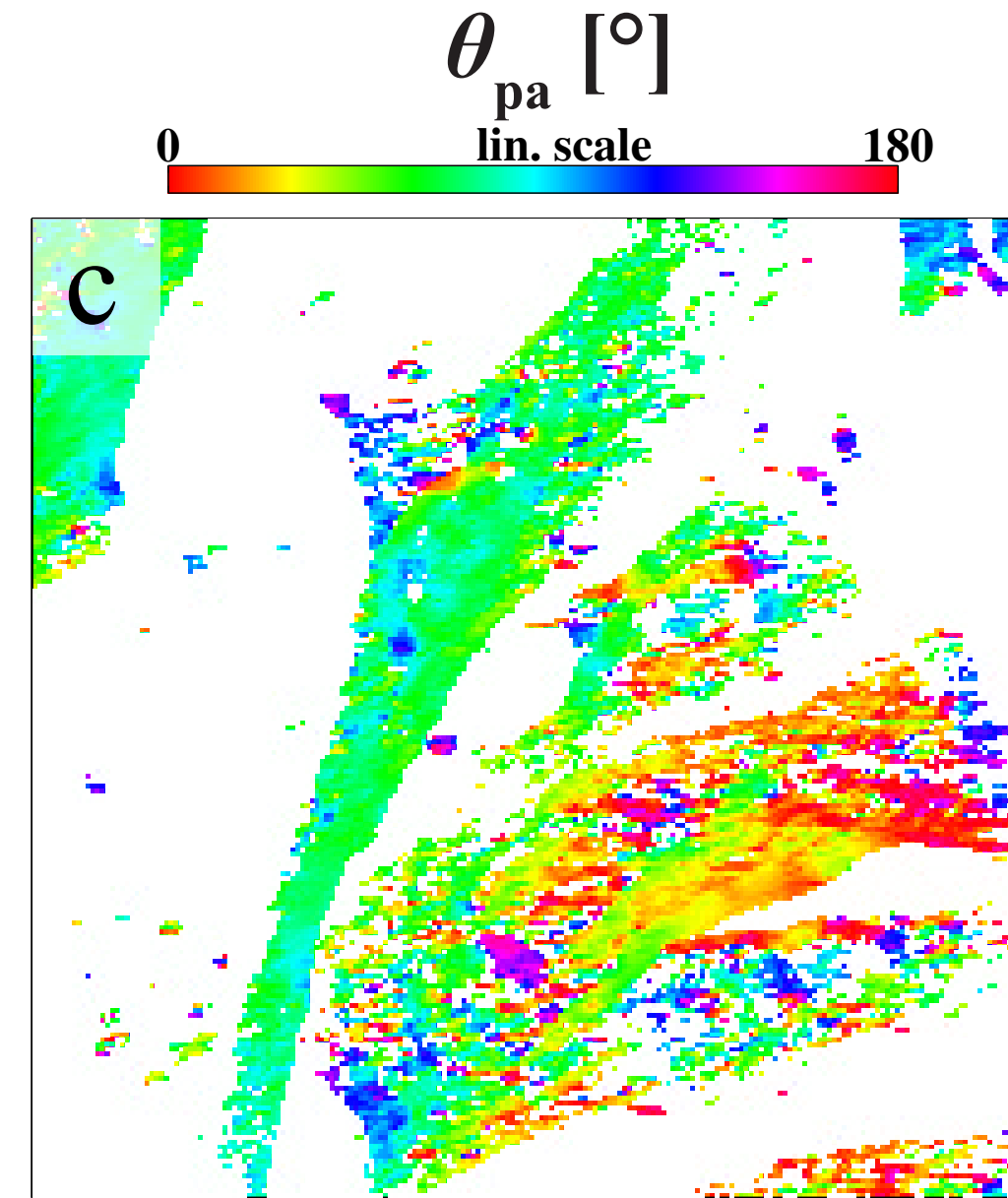
- ▶ super-structure
- ▶ length scales
- ▶ orientations

focused X-ray beam

- ▶ fixed resolution
- ▶ high dose

super resolution

- ▶ quantify structures smaller than beam size



external animation

Introduction: Methods & Algorithms

Waveguide Alignment

- ▶
- ▶
- ▶
- ▶

Measurement

- ▶
- ▶
- ▶

Pre-processing

- ▶
- ▶

Reconstructions

- ▶
- ▶
- ▶

Segmentations

- ▶
- ▶
- ▶
- ▶

"Real" analysis: statistics on segmented objects

- ▶
- ▶
- ▶
- ▶
- ▶

Introduction: Methods & Algorithms

Waveguide Alignment

- ▶ pre-align via Laser
- ▶ goto intensity maximum
- ▶ rotate by hand
- ▶ before measurements: goto intensity maximum

Measurement

- ▶ hand-crafted macros
- ▶ modular macros // TODO
- ▶ semi-automatic pre-analysis scripts

Pre-processing

- ▶ reading, cropping, masking
- ▶ flat-field correction

Reconstructions

- ▶
- ▶
- ▶

Segmentations

- ▶
- ▶
- ▶
- ▶

"Real" analysis: statistics on segmented objects

- ▶
- ▶
- ▶
- ▶
- ▶

Introduction: Methods & Algorithms

Waveguide Alignment

- ▶ pre-align via Laser
- ▶ goto intensity maximum
- ▶ rotate by hand
- ▶ before measurements: goto intensity maximum

Measurement

- ▶ hand-crafted macros
- ▶ modular macros // TODO
- ▶ semi-automatic pre-analysis scripts

Pre-processing

- ▶ reading, cropping, masking
- ▶ alignment
- ▶ flat-field correction

Reconstructions

- ▶ holographic reconstruction (ill-posed)
- ▶ tomographic reconstruction (inverse Radon)
- ▶ → grey values in cylinder → 3D electron density distribution

Segmentations

- ▶ grey-value based
- ▶ local histogram
- ▶ gradients, edges etc.
- ▶ AI based: train by hand (e.g. drawing objects)

“Real” analysis: statistics on segmented objects

- ▶ cells' size, mass, shape, orientation, density
- ▶ distance to next neighbour, to other objects
- ▶ connectedness (neurons)
- ▶ compare histograms, CTRL vs. DISEASE / TREATMENT
- ▶ ...

Where AI could/might/does help

Accelerator



Beamline / instrument

- ▶ design
- ▶ alignment

Measurement

- ▶ stability etc.
- ▶ data quality
- ▶ data rejection

Pre-processing

- ▶ image rejection
- ▶ alignment
- ▶ flat-field correction

Reconstructions

- ▶ holo, tomo
- ▶ incoming projection → tomo
-

Segmentation

-
-
- ▶
- ▶

"Real" analysis

-
-
- ▶
- ▶

Introduction: AI

Accelerator

design

operation

Beamline / instrument

▶ design

▶ alignment

Measurement

▶ stability etc.

▶ data quality

▶ data rejection

Pre-processing

▶ image rejection

▶ alignment

▶ flat-field correction

Reconstructions

▶ holo, tomo

▶ incoming projection → tomo

missing wedge

Segmentation

find pre-trained objects

find user-trained objects

▶ fully automated pipeline

▶ pre-trained networks

"Real" analysis

compare histograms

classify healthy/disease

▶ pre-clinical research

▶ diagnostic research

Virtual Patho-Histology at the GINIX 3D X-ray Microscope

Markus Osterhoff
Institut für Röntgenphysik,
Uni Göttingen

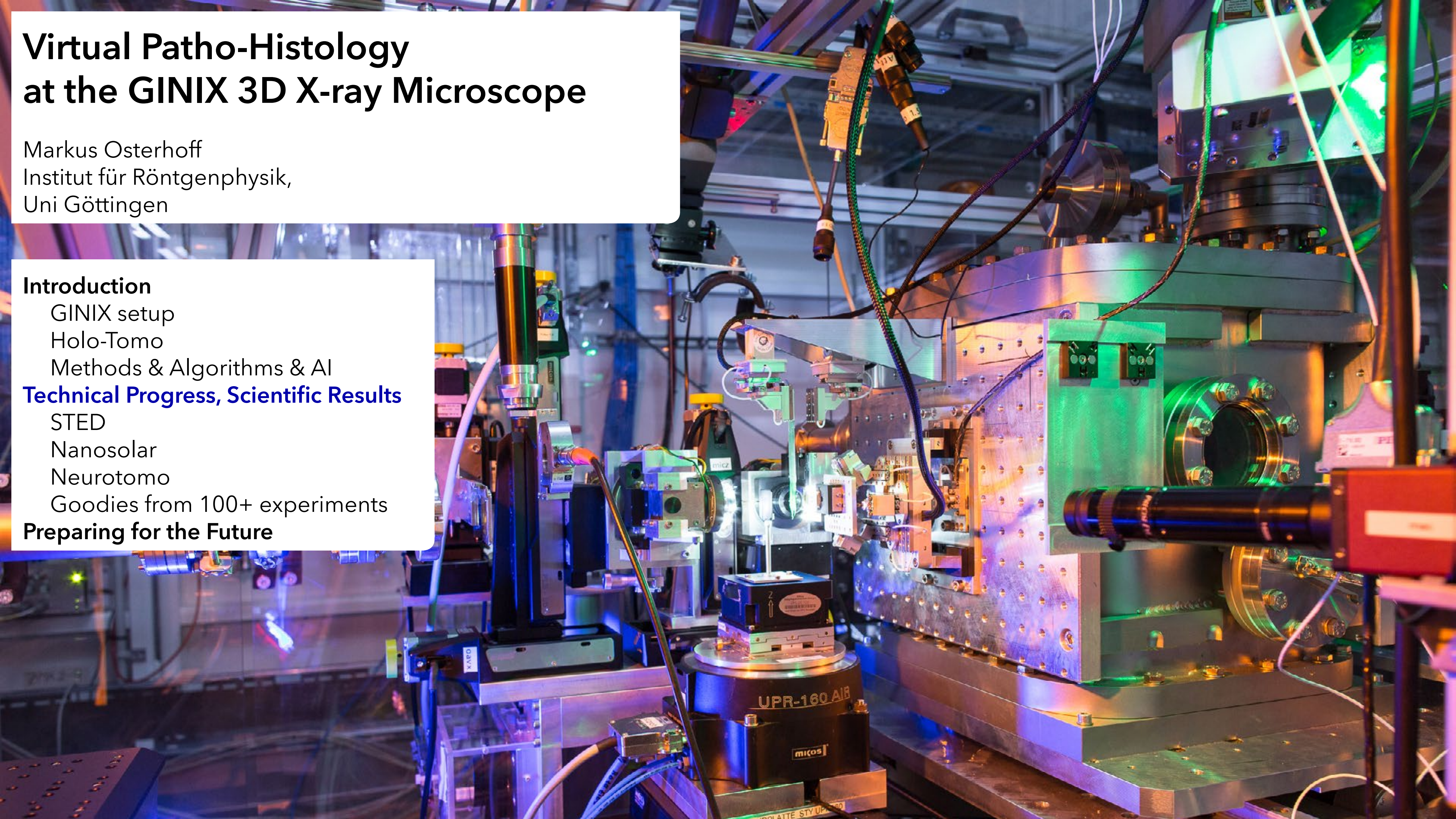
Introduction

GINIX setup
Holo-Tomo
Methods & Algorithms & AI

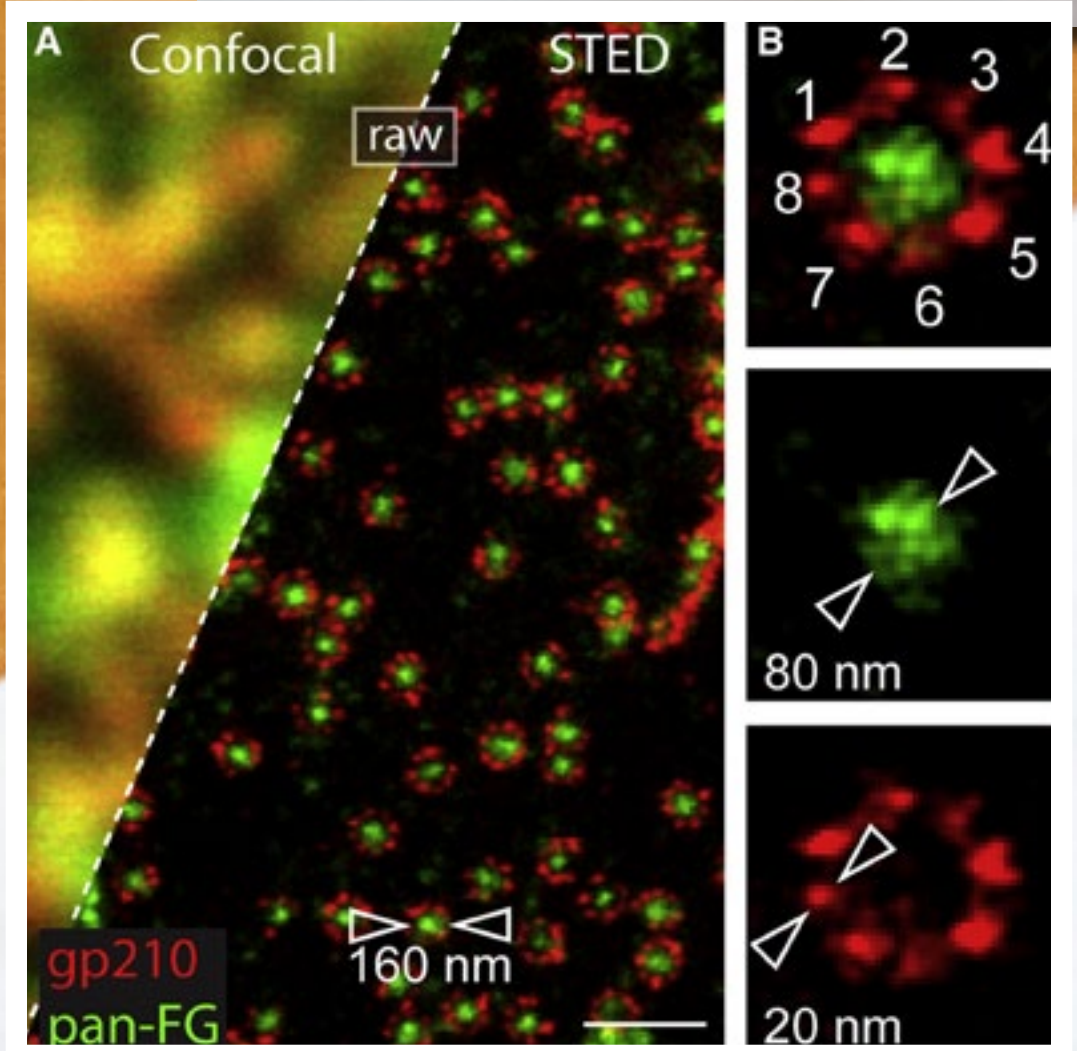
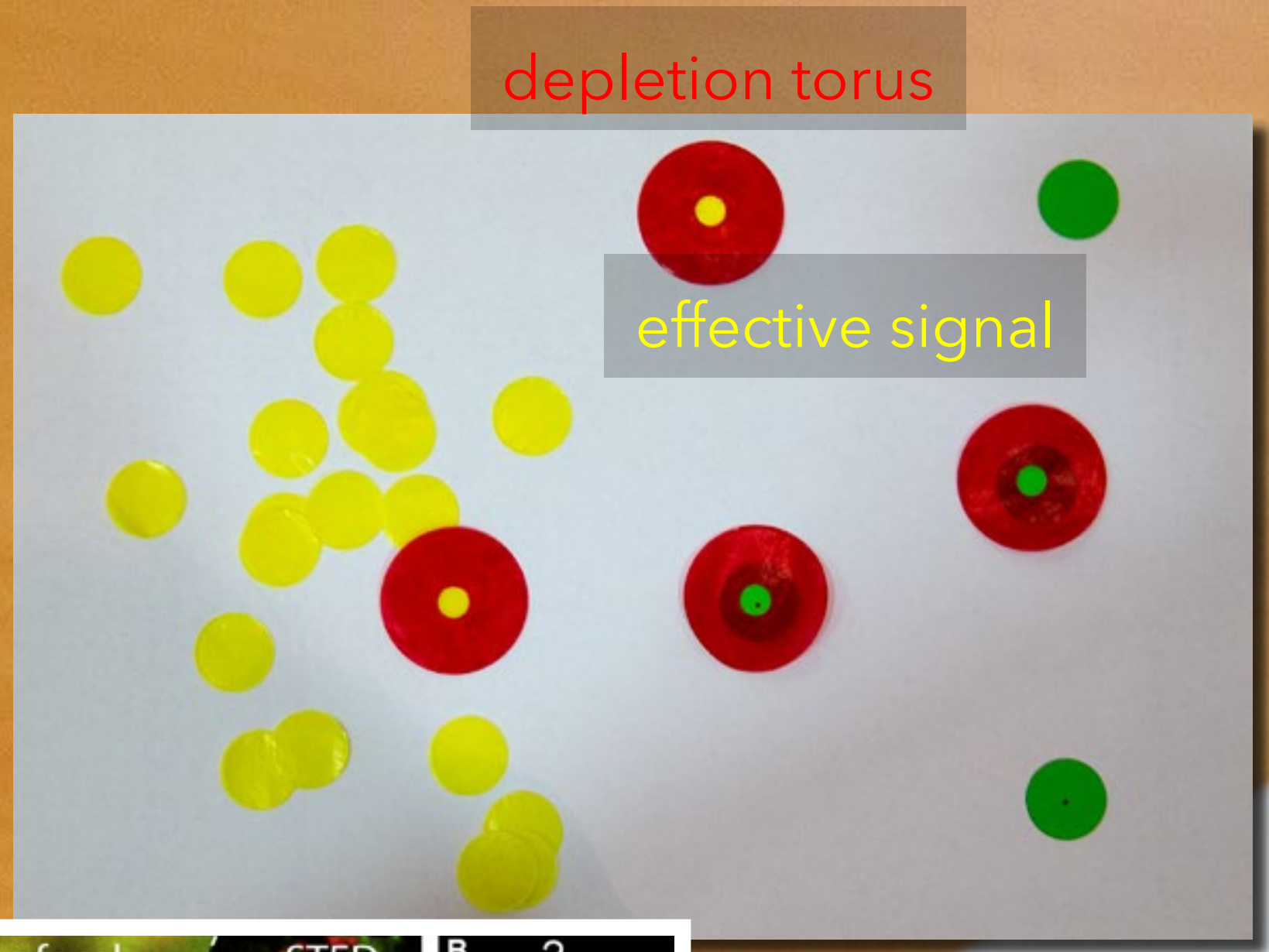
Technical Progress, Scientific Results

STED
Nanosolar
Neurotomo
Goodies from 100+ experiments

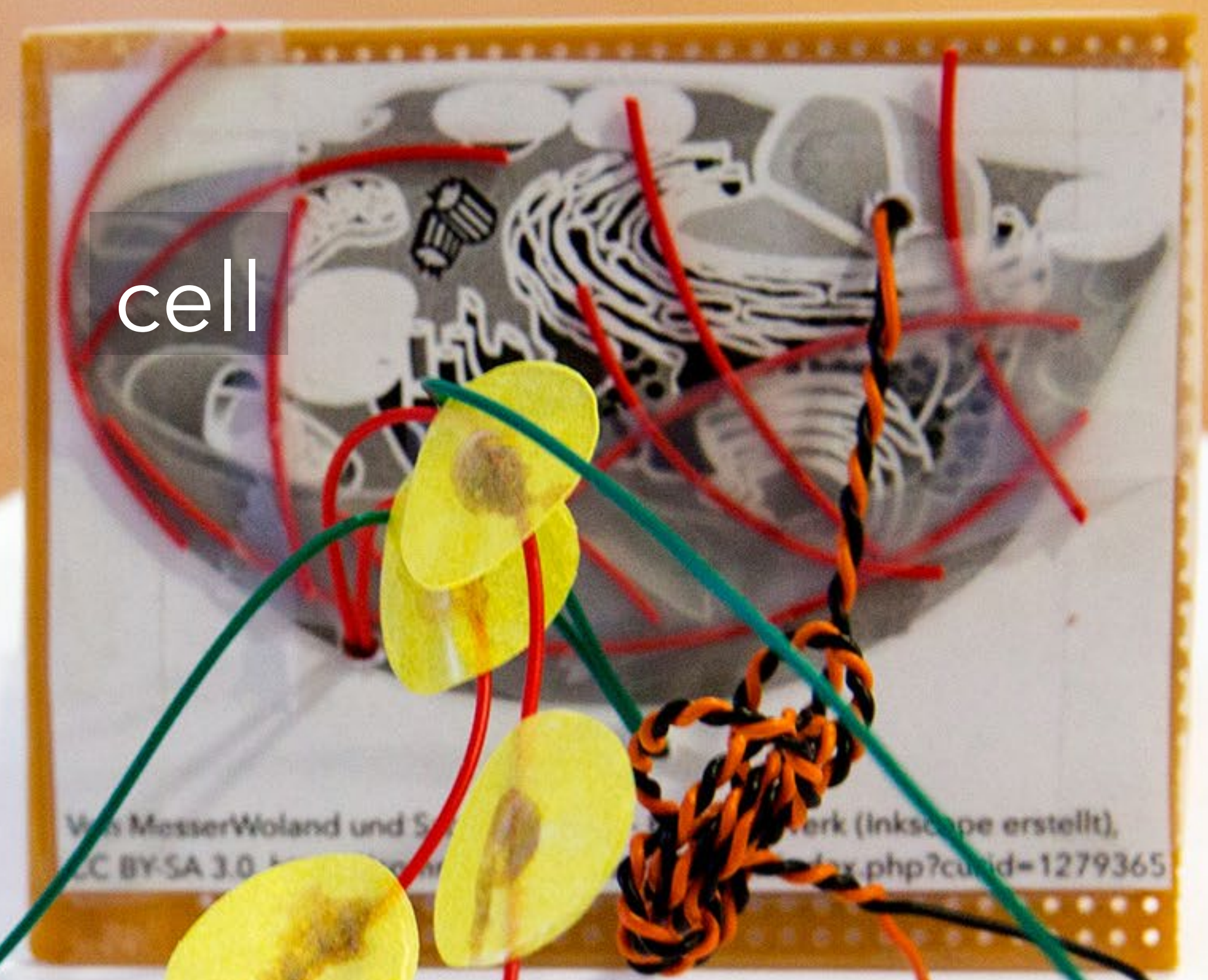
Preparing for the Future



Progress & Results: STED



Stefan Hell et al.,
Biophys J, 2013



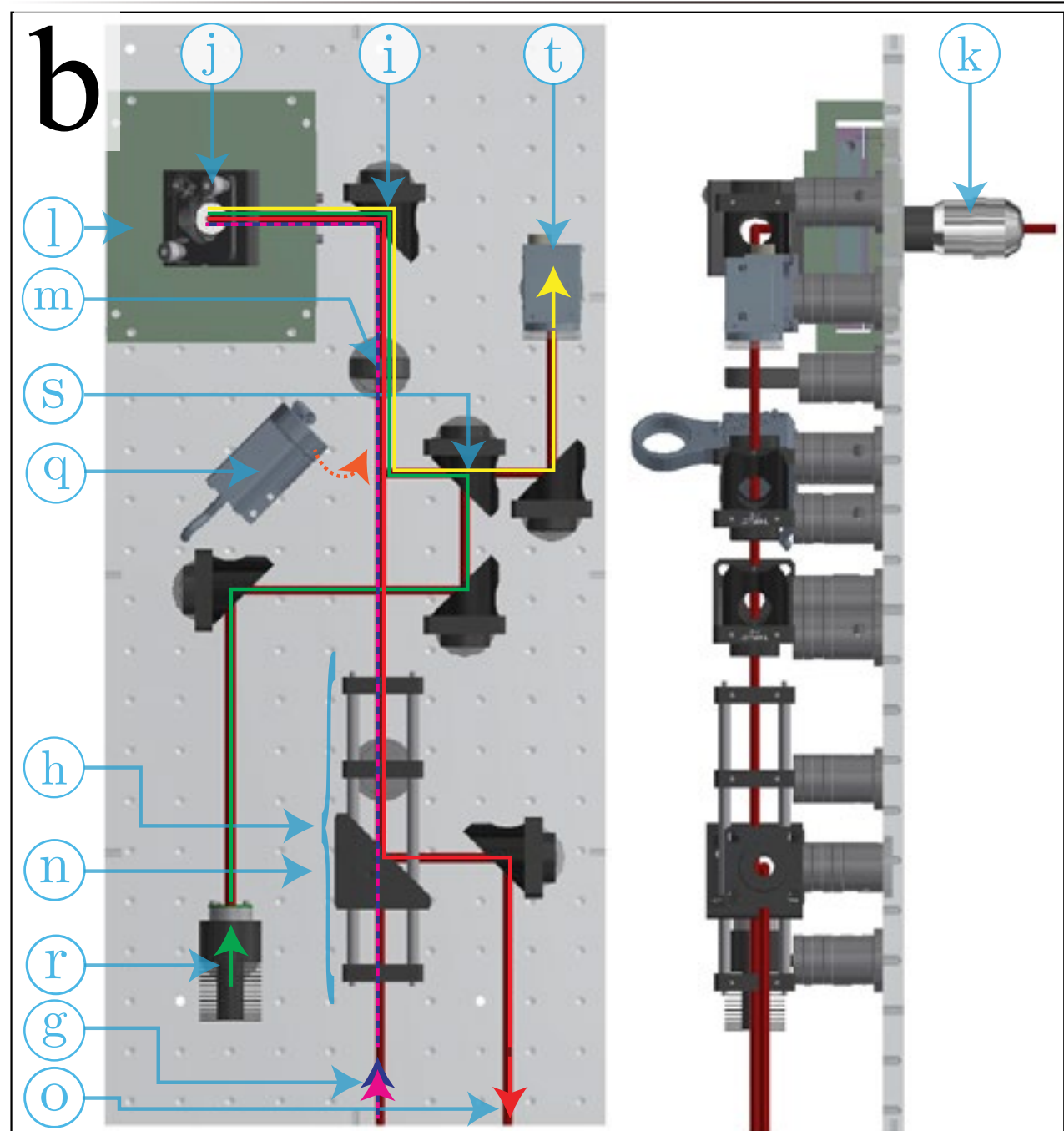
another kind of fibre

specific glue

diffraction limited spot of fluorophore

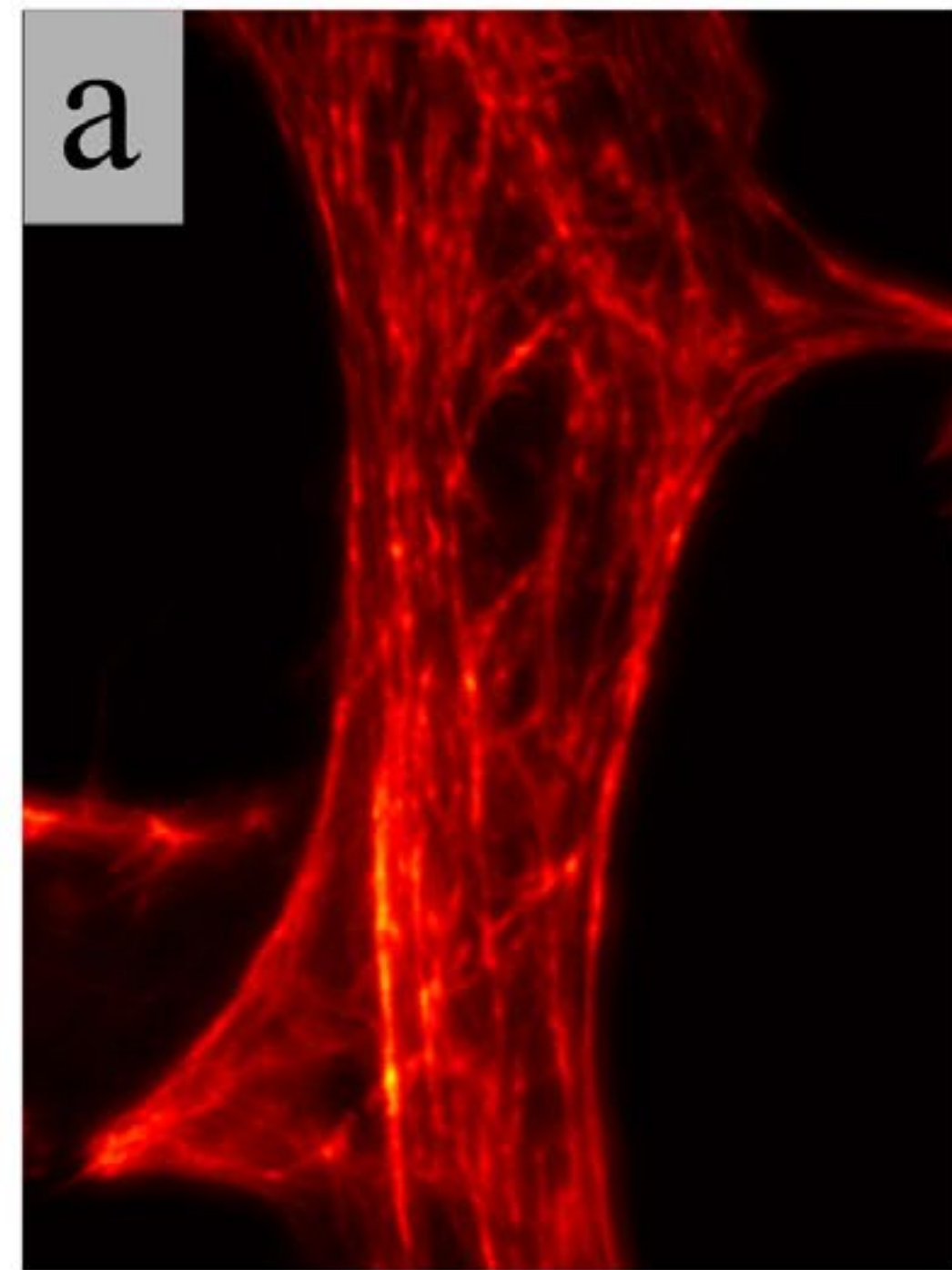
fibre of interest

Progress & Results: STED



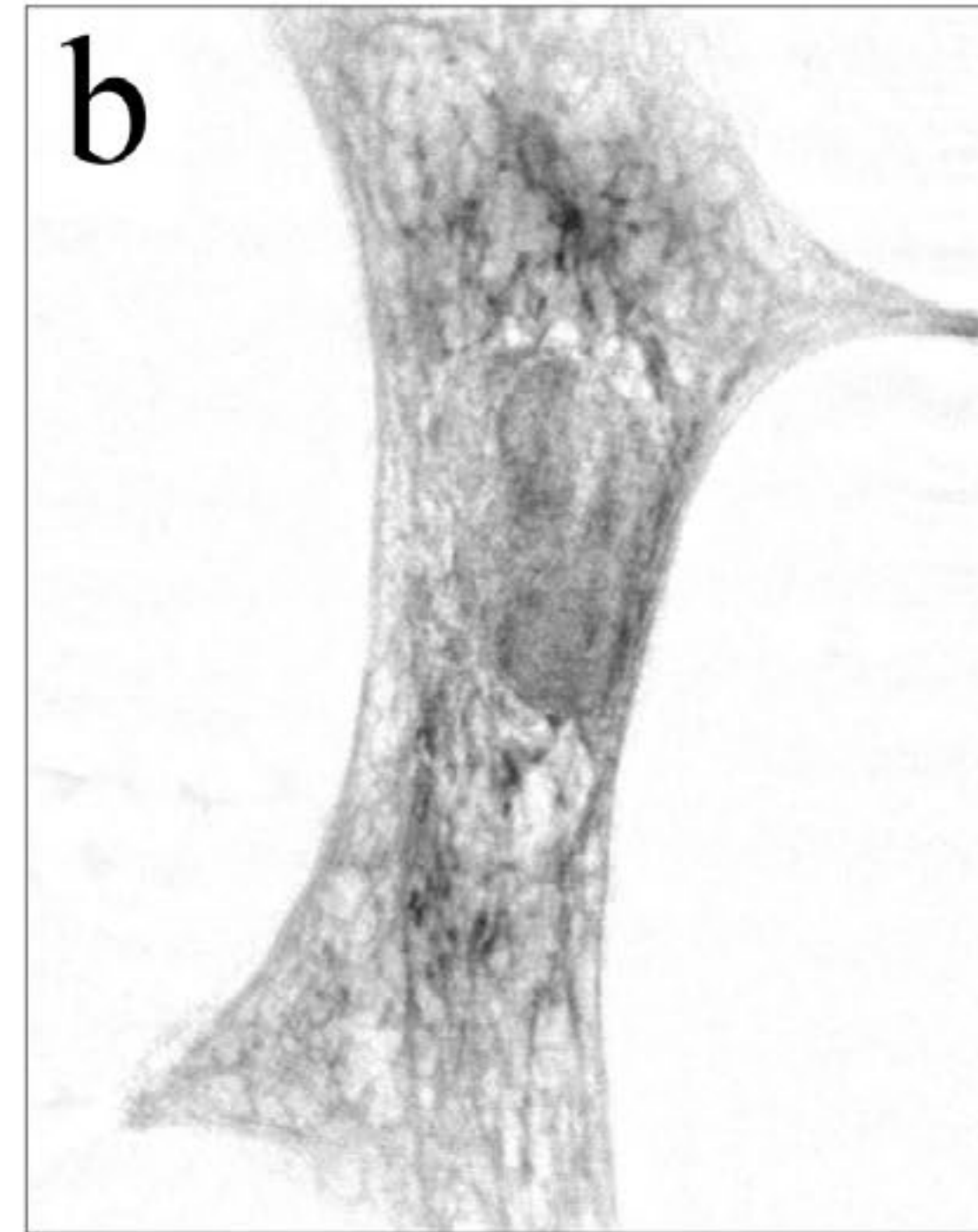
STED fluorescence

I [ph./s]
lin. scale
0.00E0 1.50E7



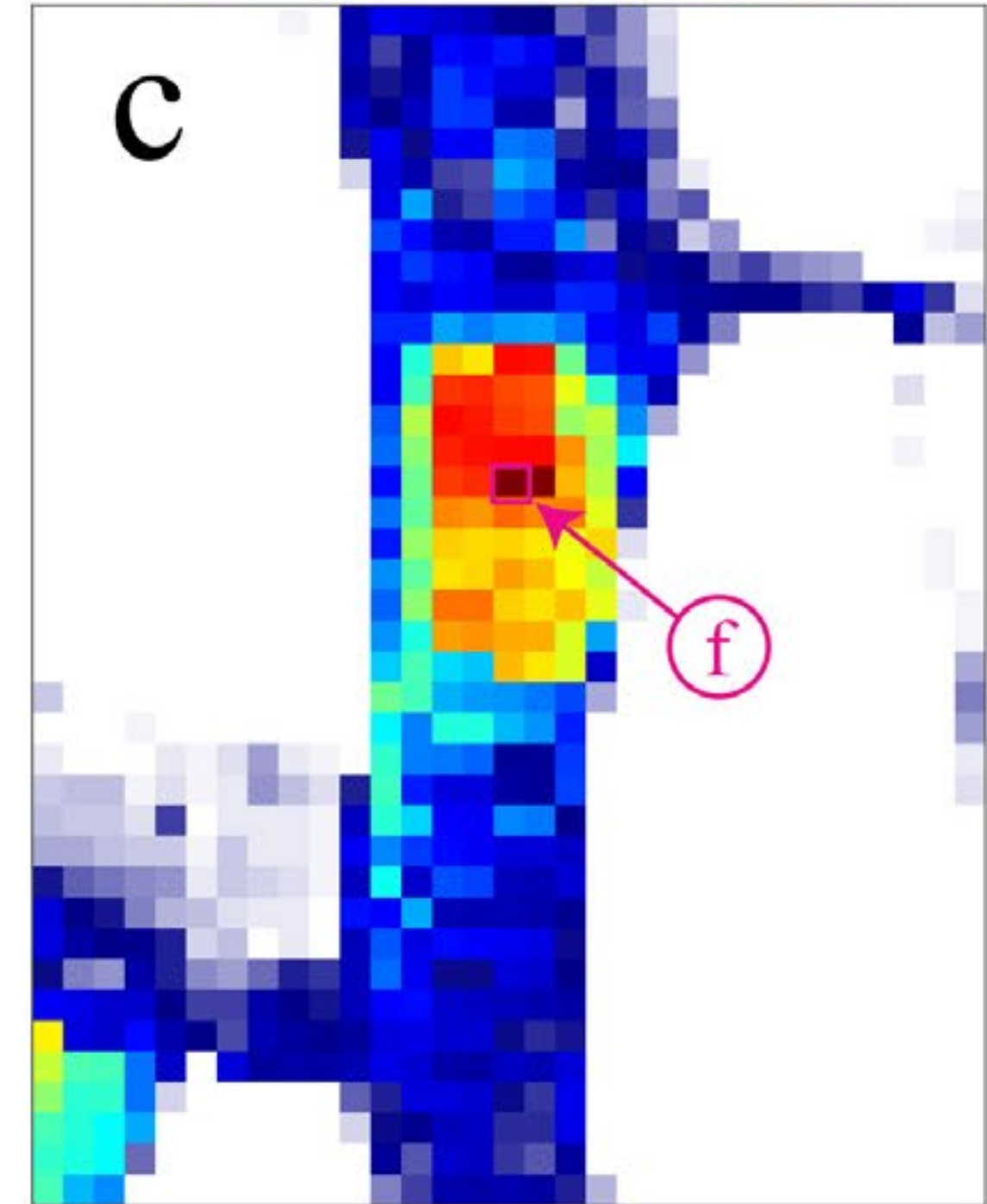
X-ray hologram

ϕ [°]
lin. scale
-0.07 0.00



X-ray nano-SAXS

I [ph./s]
lin. scale
6.50E5 2.90E6

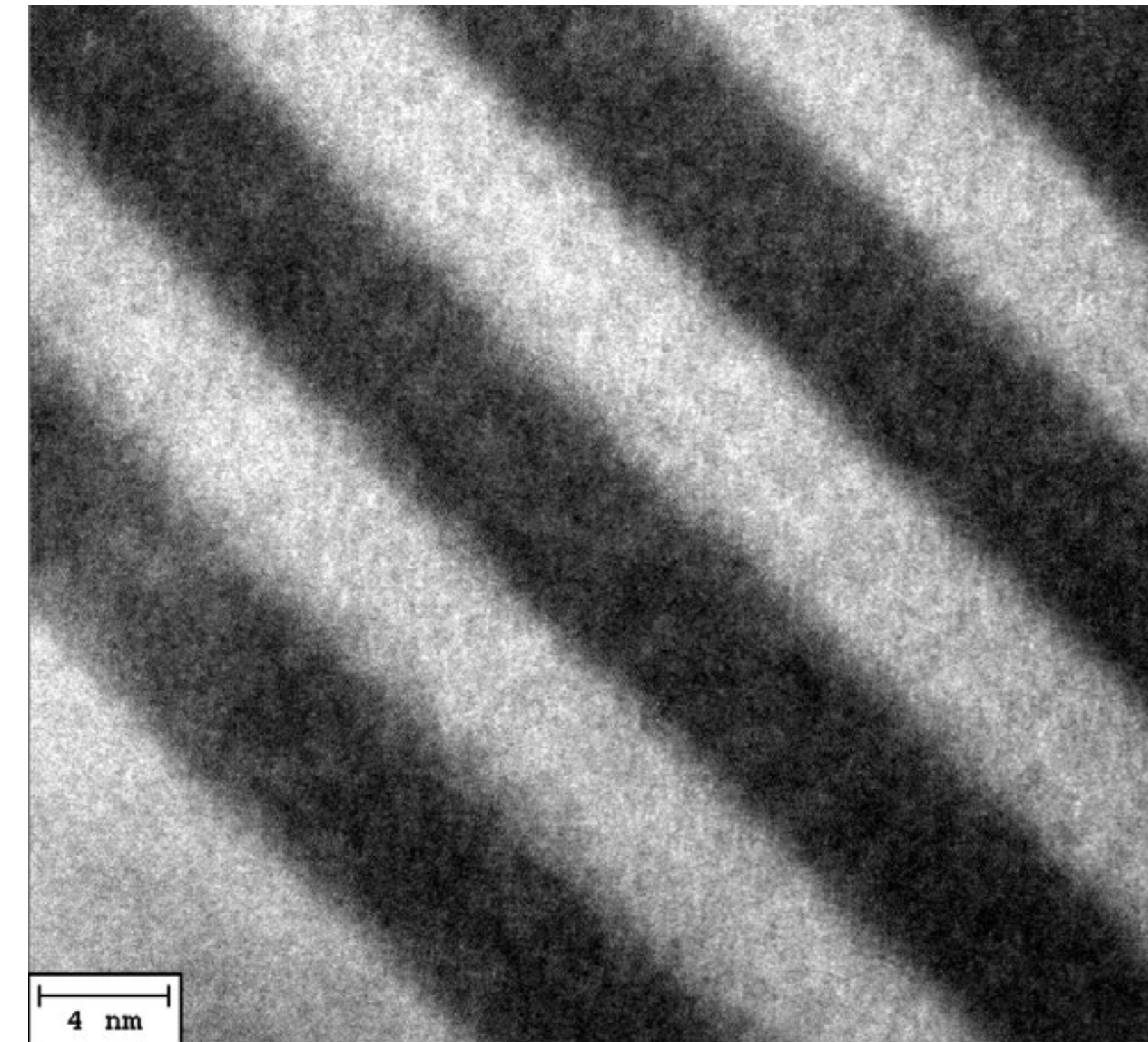
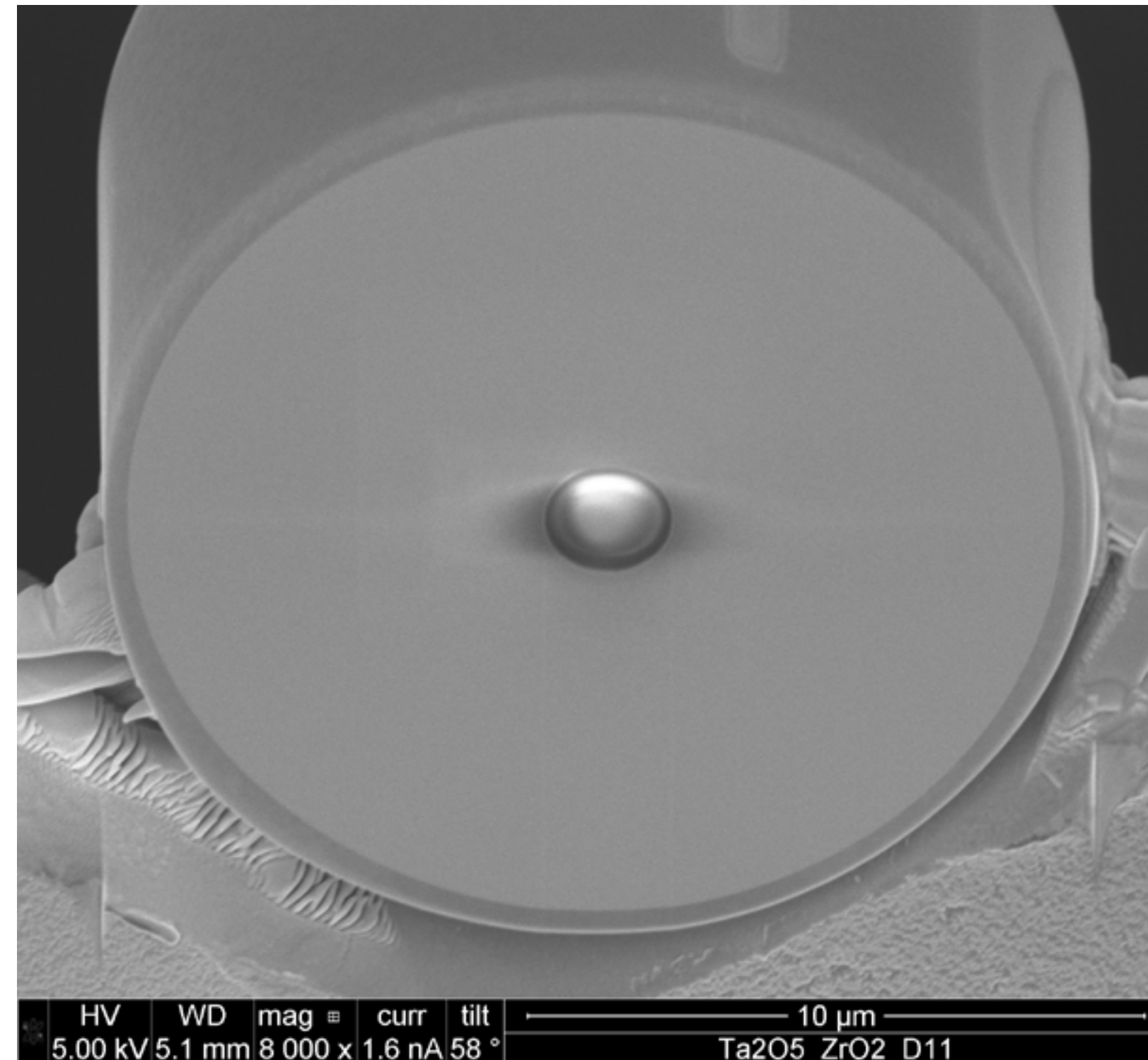
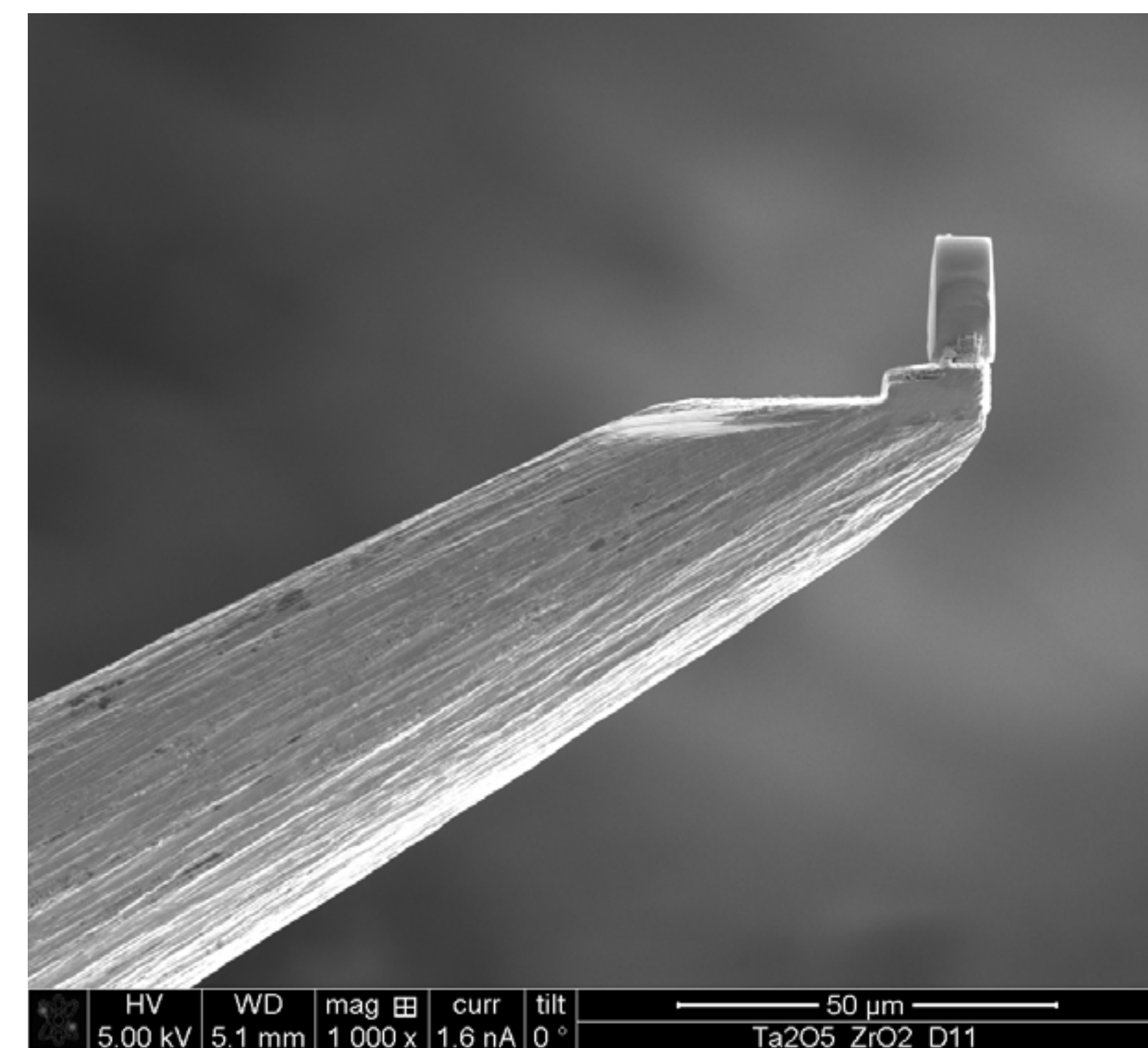
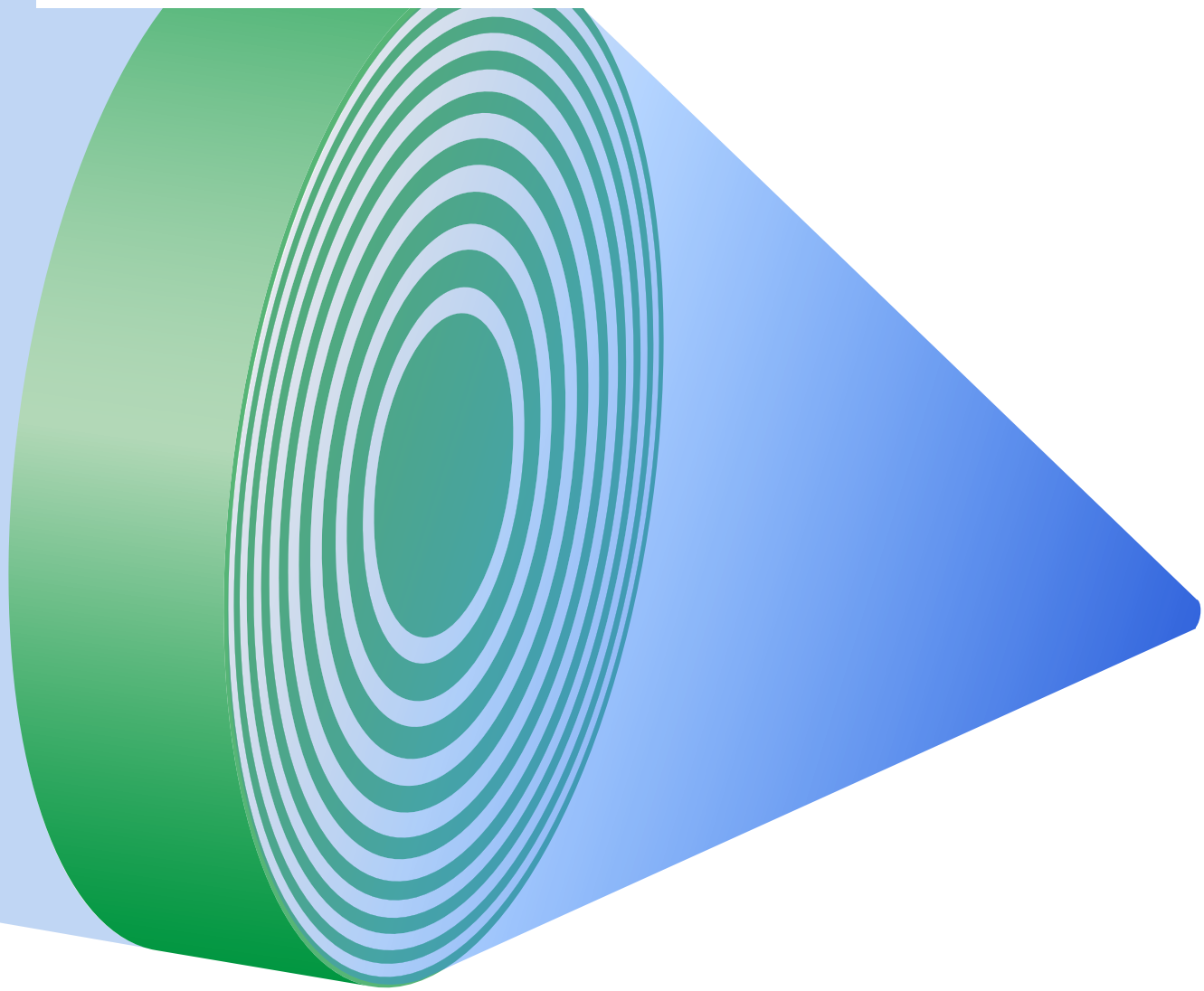


Marten Bernhardt, Sarah Köster, Tim Salditt *et al.*
Nature Communications, 2018

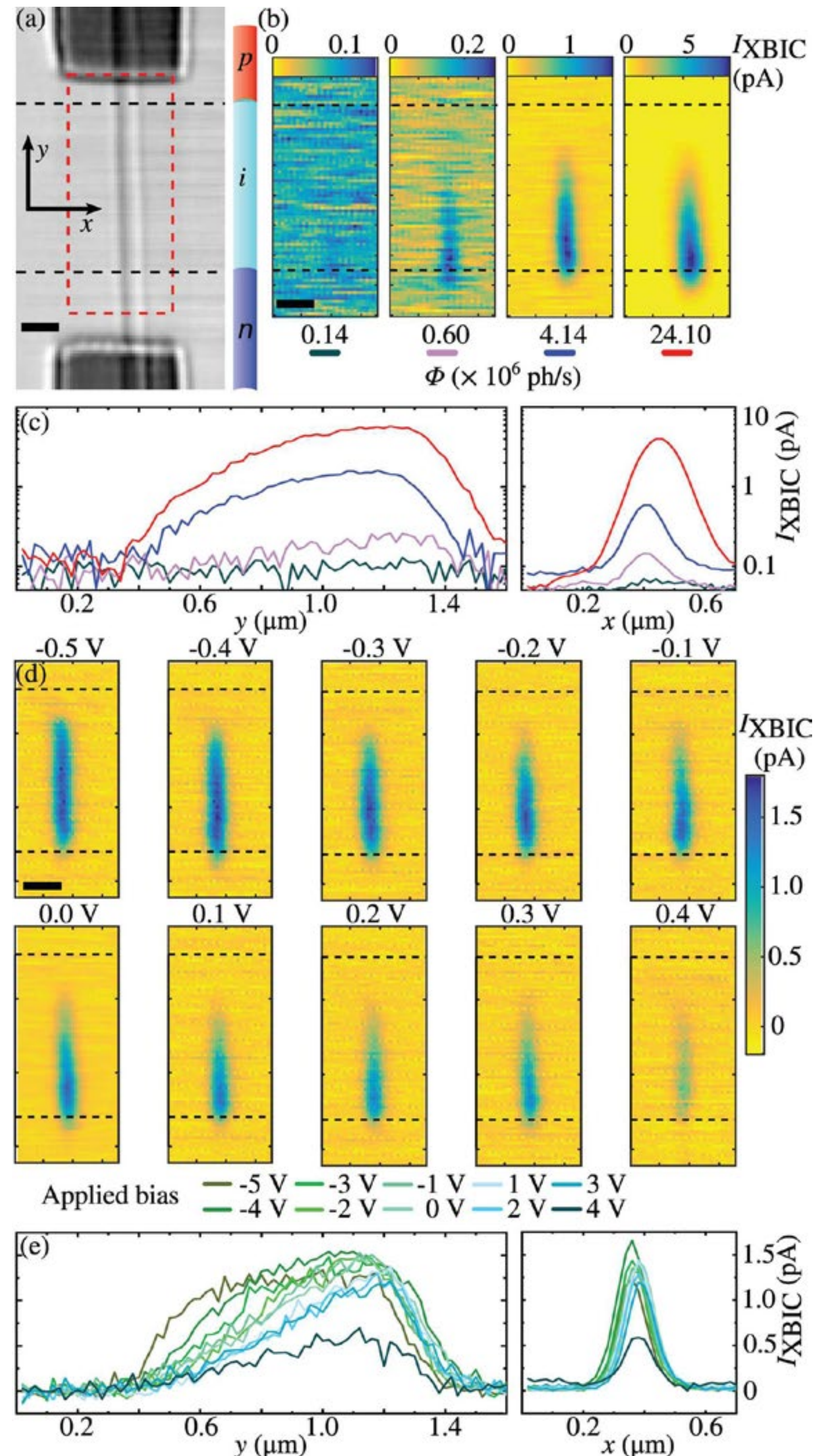
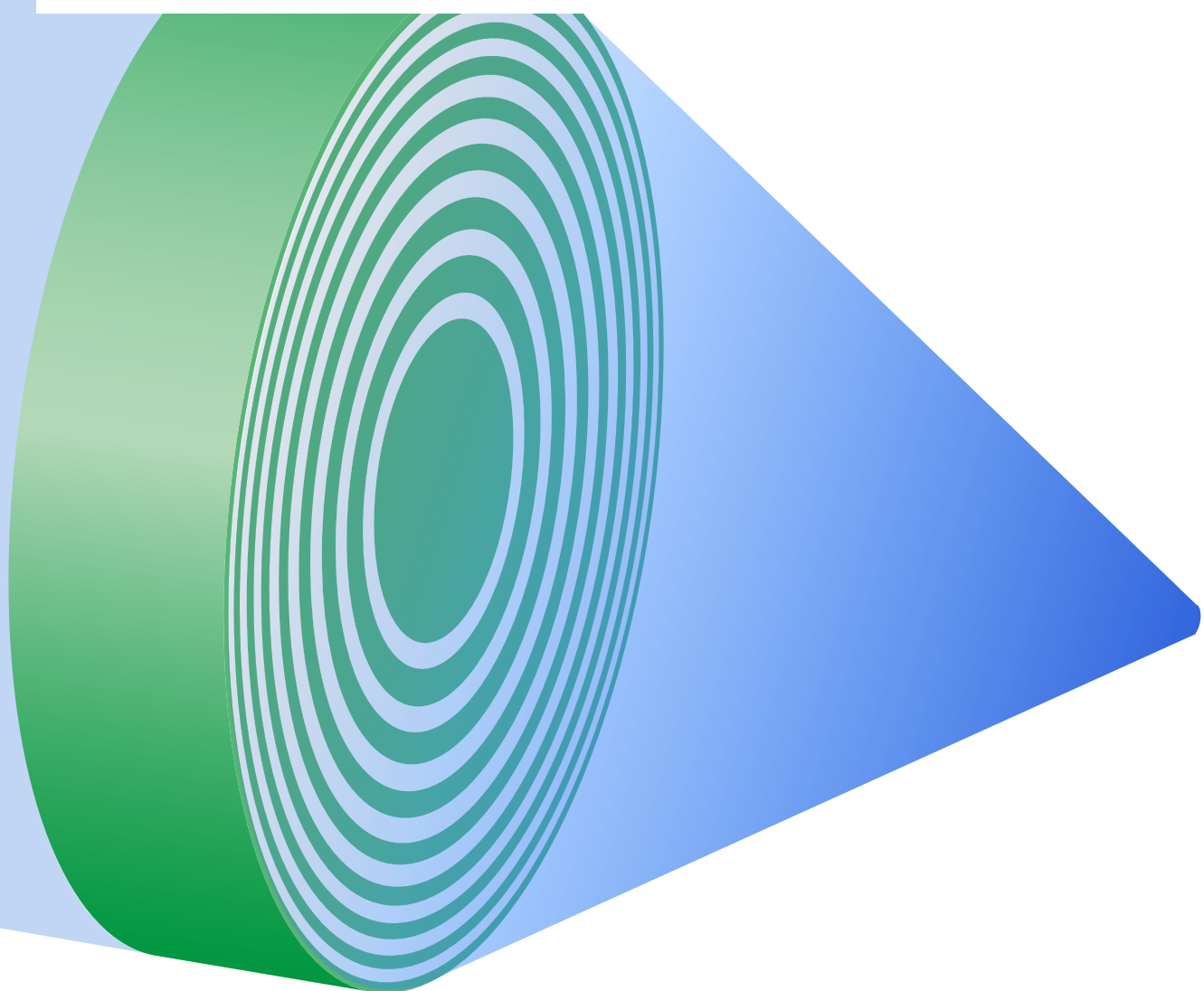
Multilayer Zone Plates

for hard X-rays @ 8...100keV and 2D-focusing, ≤ 10 nm

(mo, Christian Eberl, Jakob Soltau, Jesper Wallentin, Hans-Ulrich Krebs *et al.*)



Progress & Results: Nanosolar

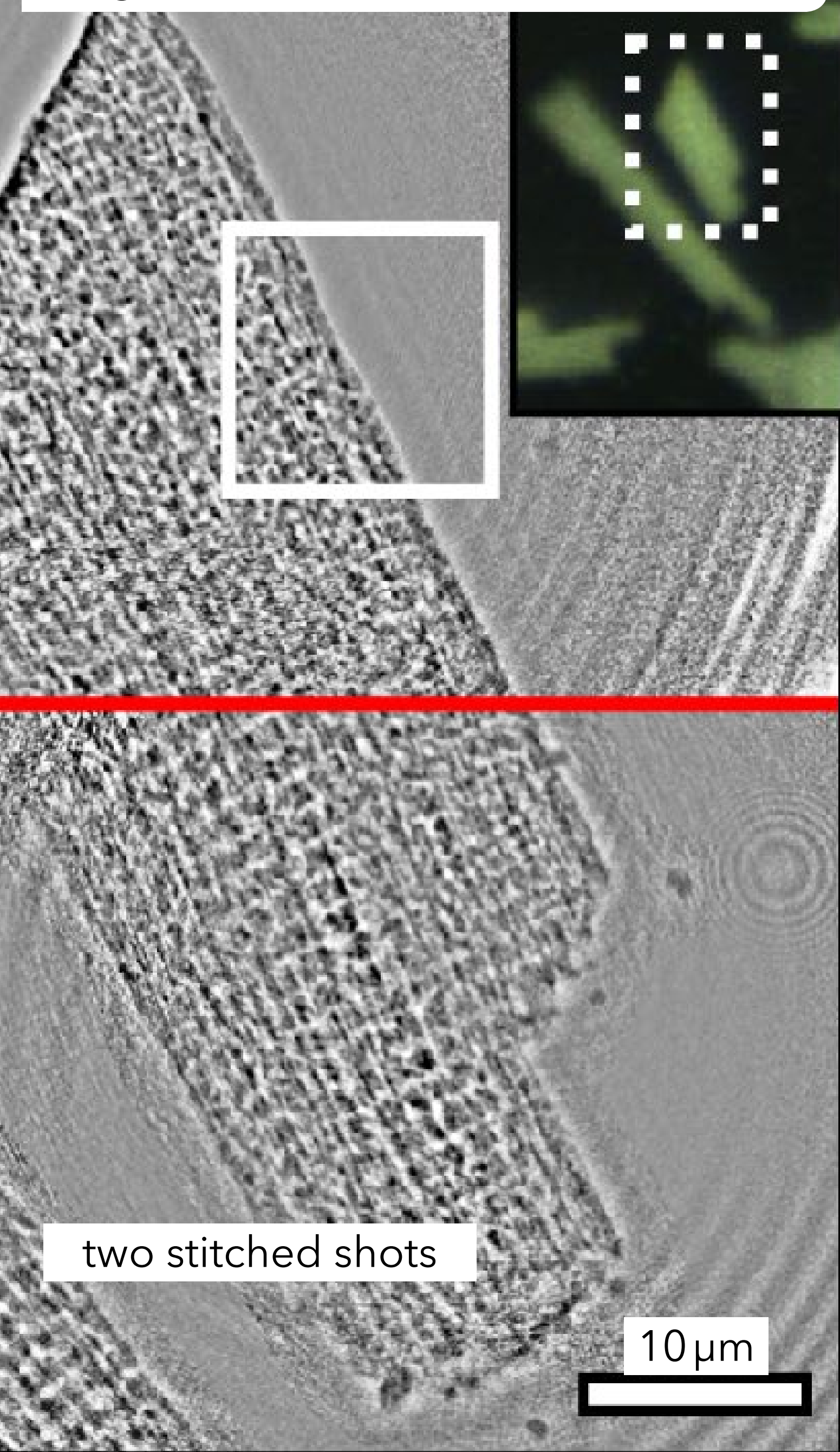


2D mapping of X-ray Beam Induced Currents

stepsize 20 nm,
scalebar 250 nm,
varying X-ray intensity (b),
varying bias voltage (d)

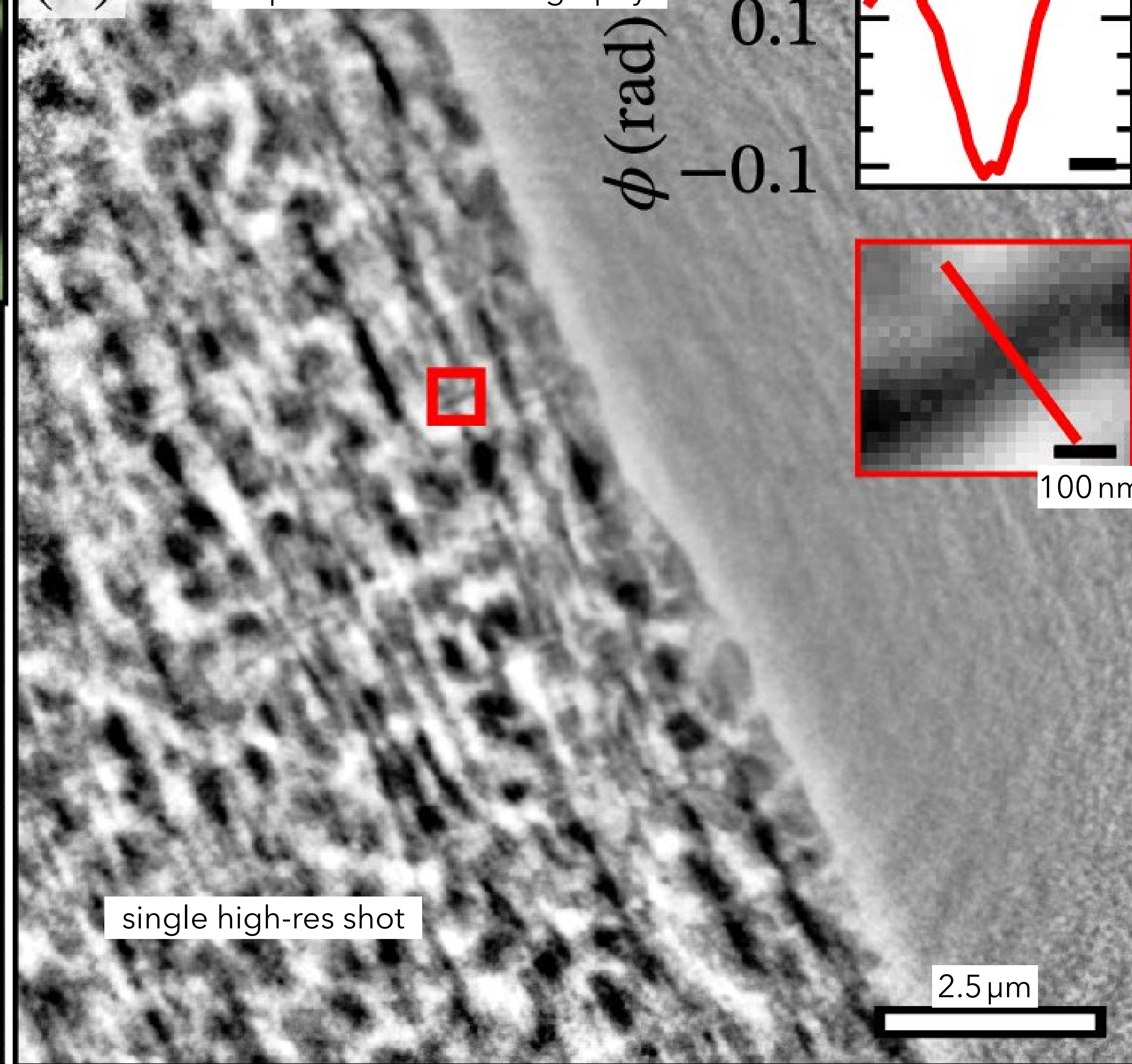
Jakob Soltau *et al.* JSR 2021

Progress & Results: Neurotomo



(b)

"Super-resolution holography"



ϕ (rad)

0.2

0.1

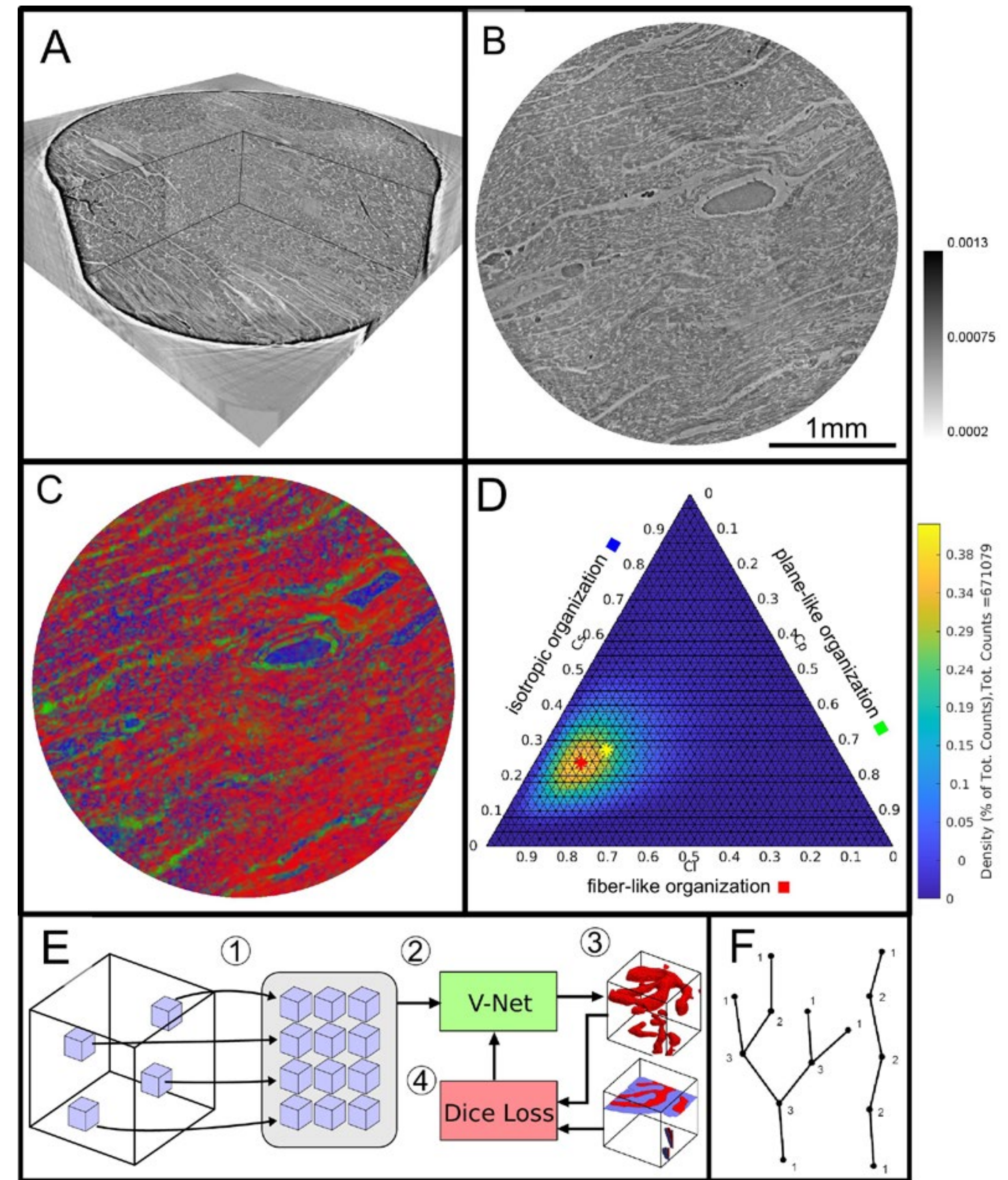
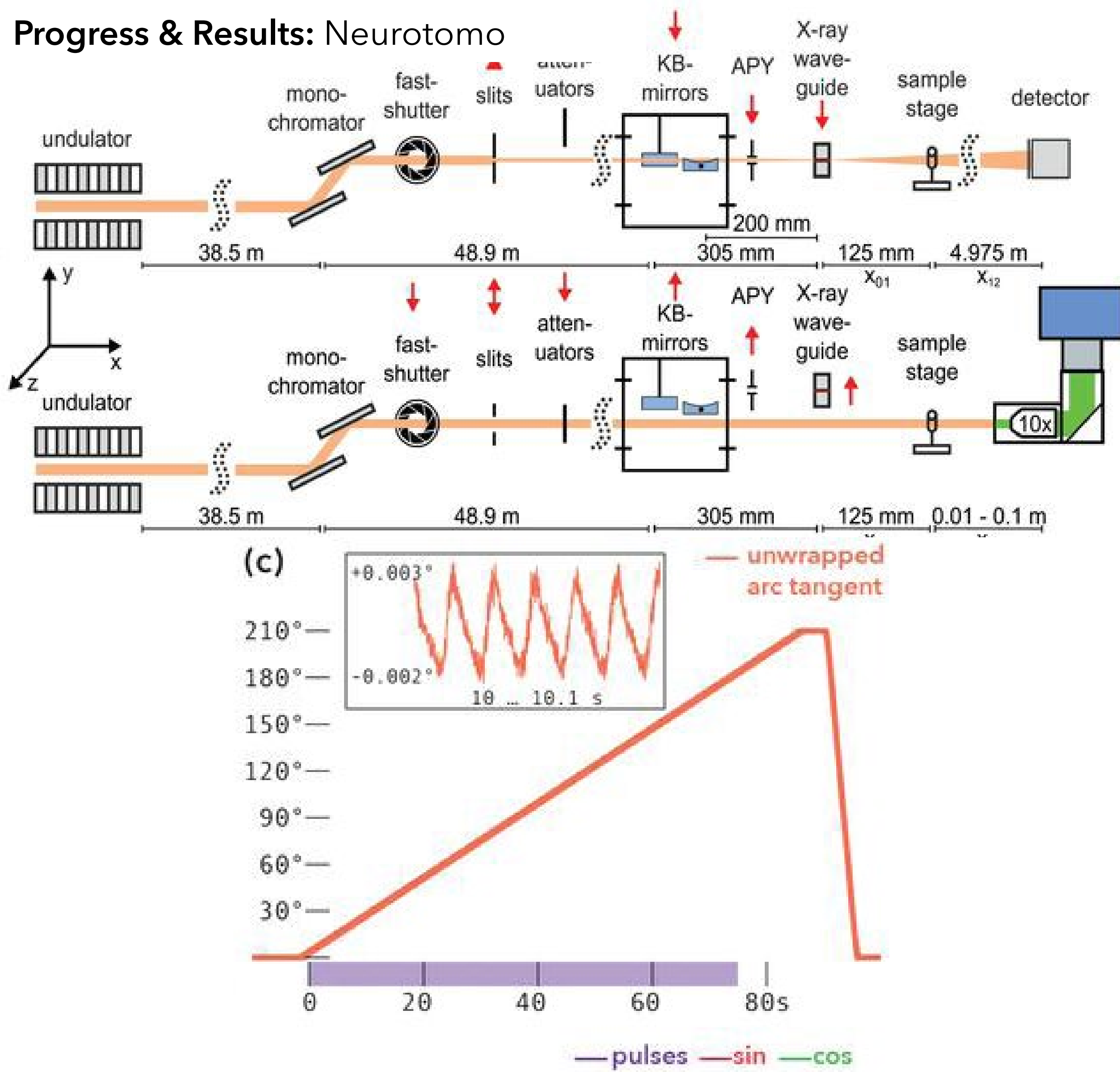
0.0

-0.1

-0.2

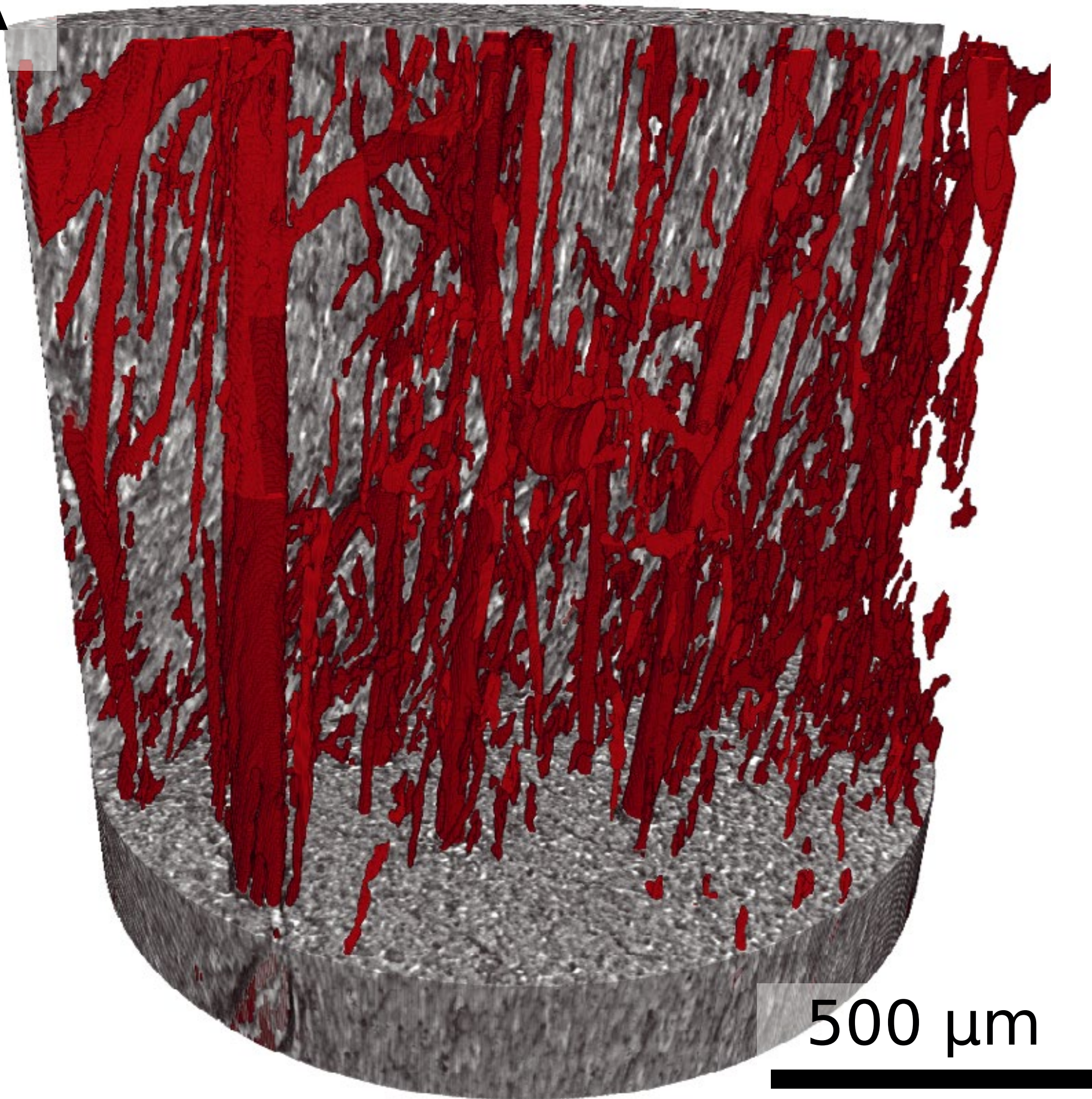
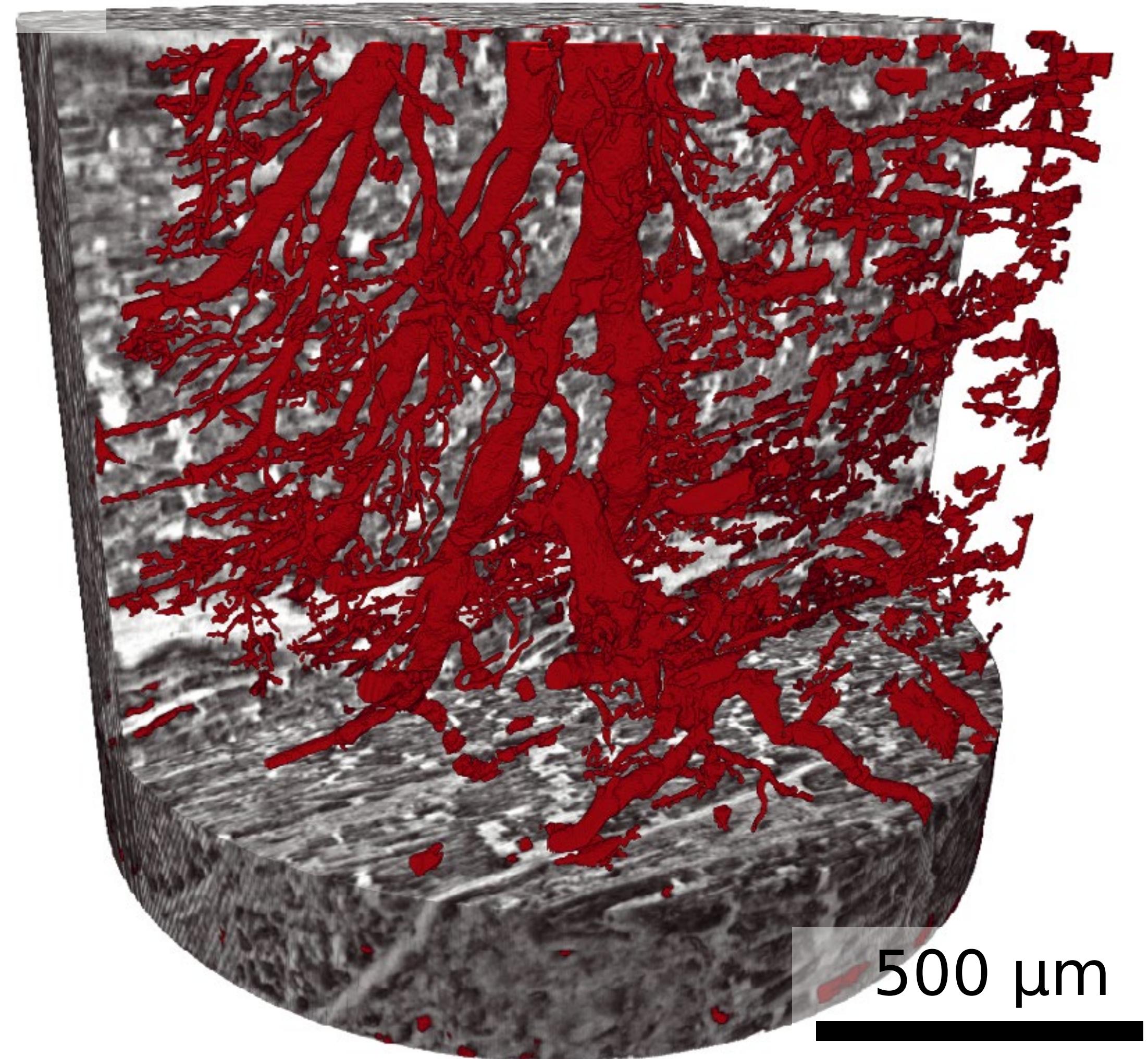
Jakob Soltau
et al.

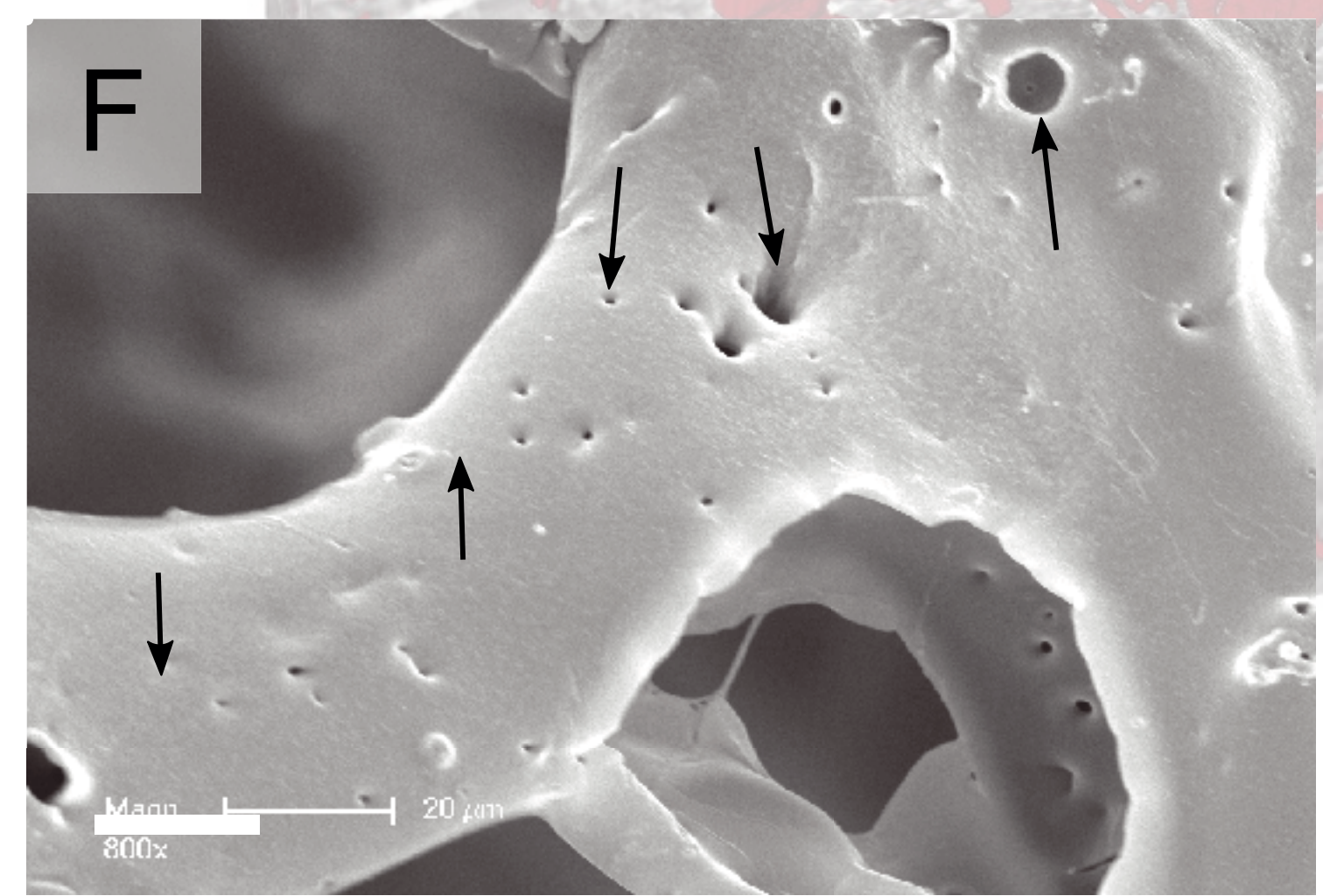
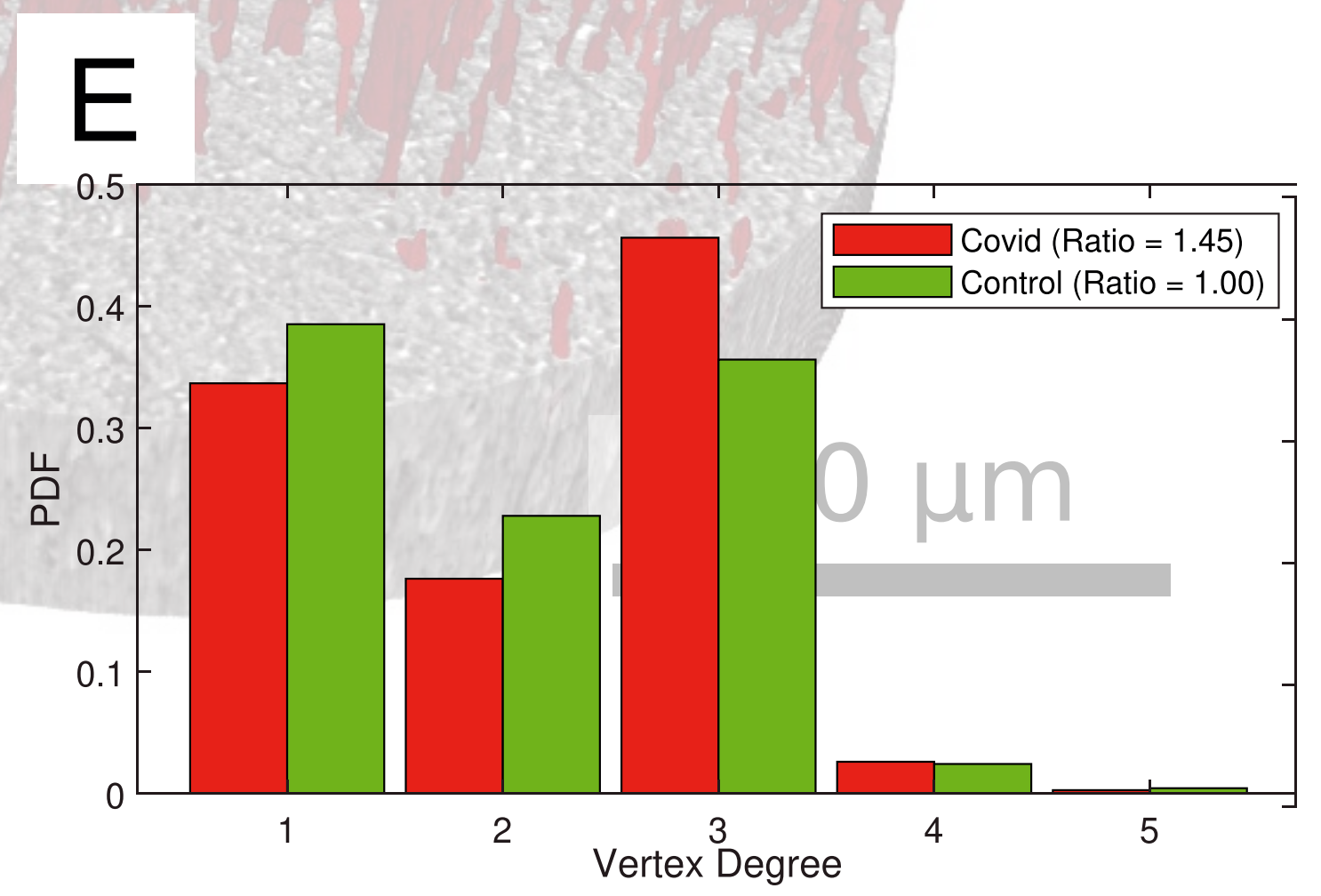
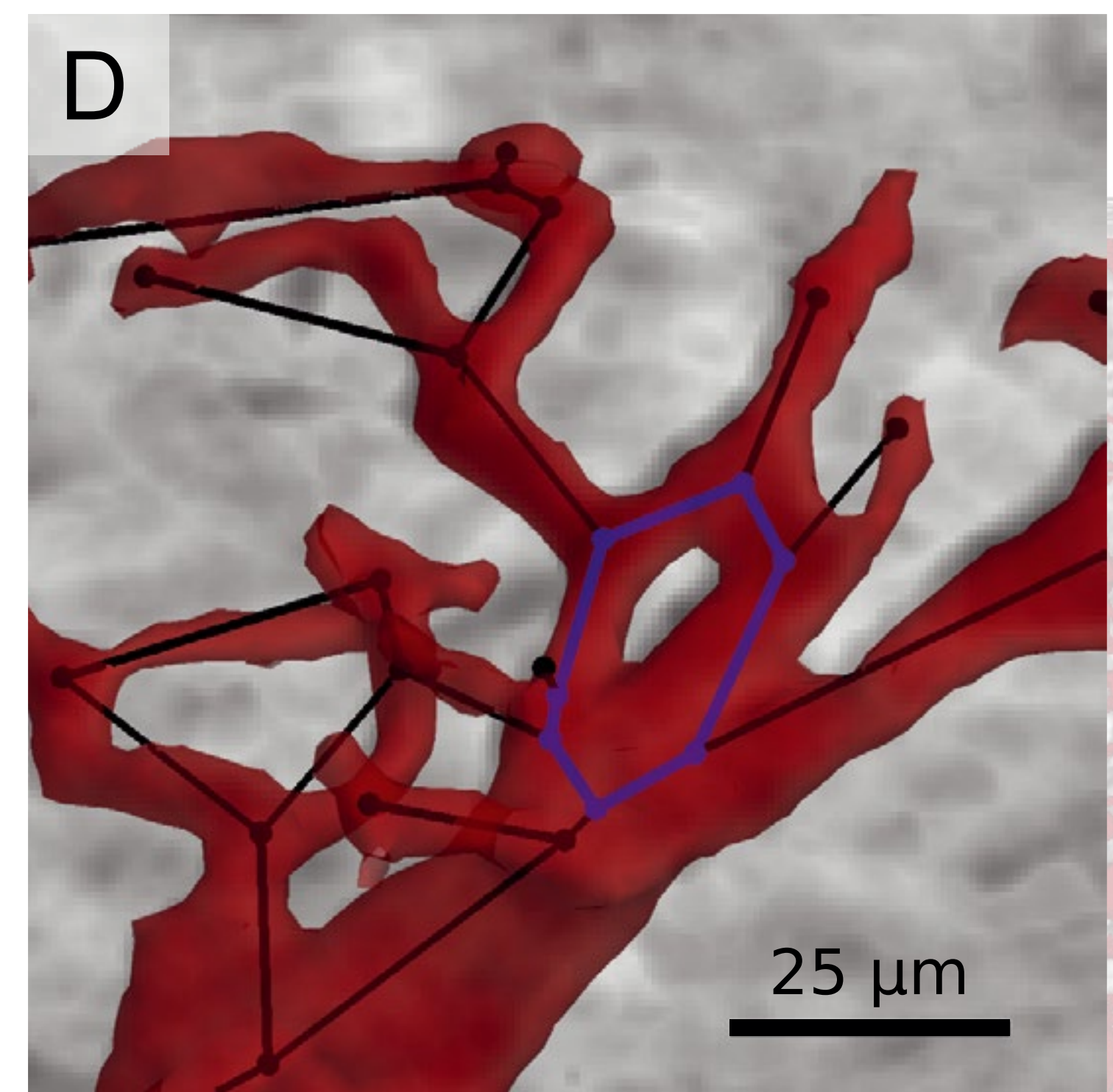
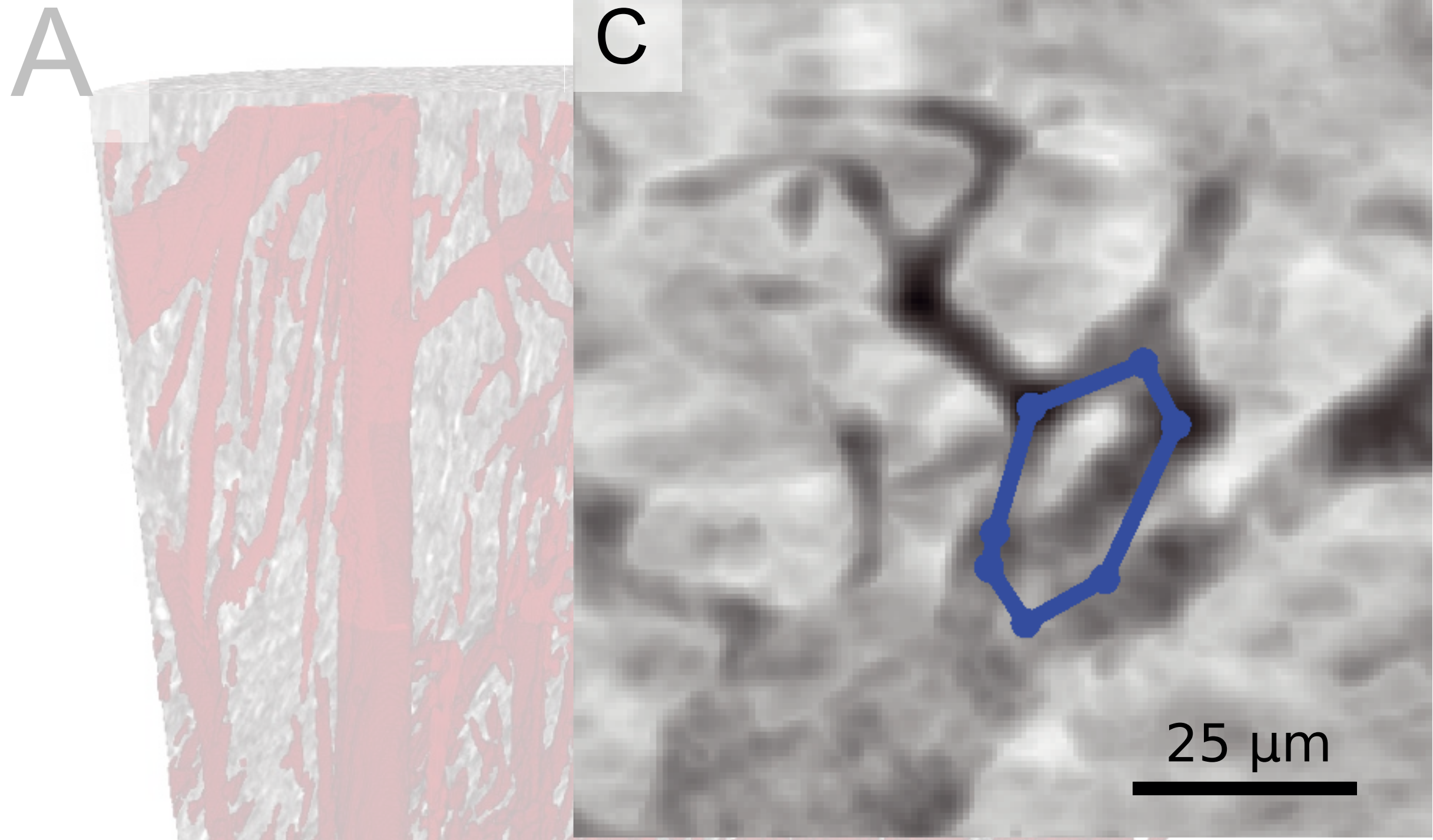
Progress & Results: Neurotomography



Jasper Frohn *et al.*: J Synchrotron Rad. 27, 1707-1719, 2020
 3D virtual histology of human pancreatic tissue
 by multiscale phase-contrast X-ray tomography

Marius Reichardt *et al.*: eLife 10:e71359, 2021
 3D virtual histopathology of cardiac tissue from
 Covid-19 patients based on phase-contrast X-ray tomography

A**B**

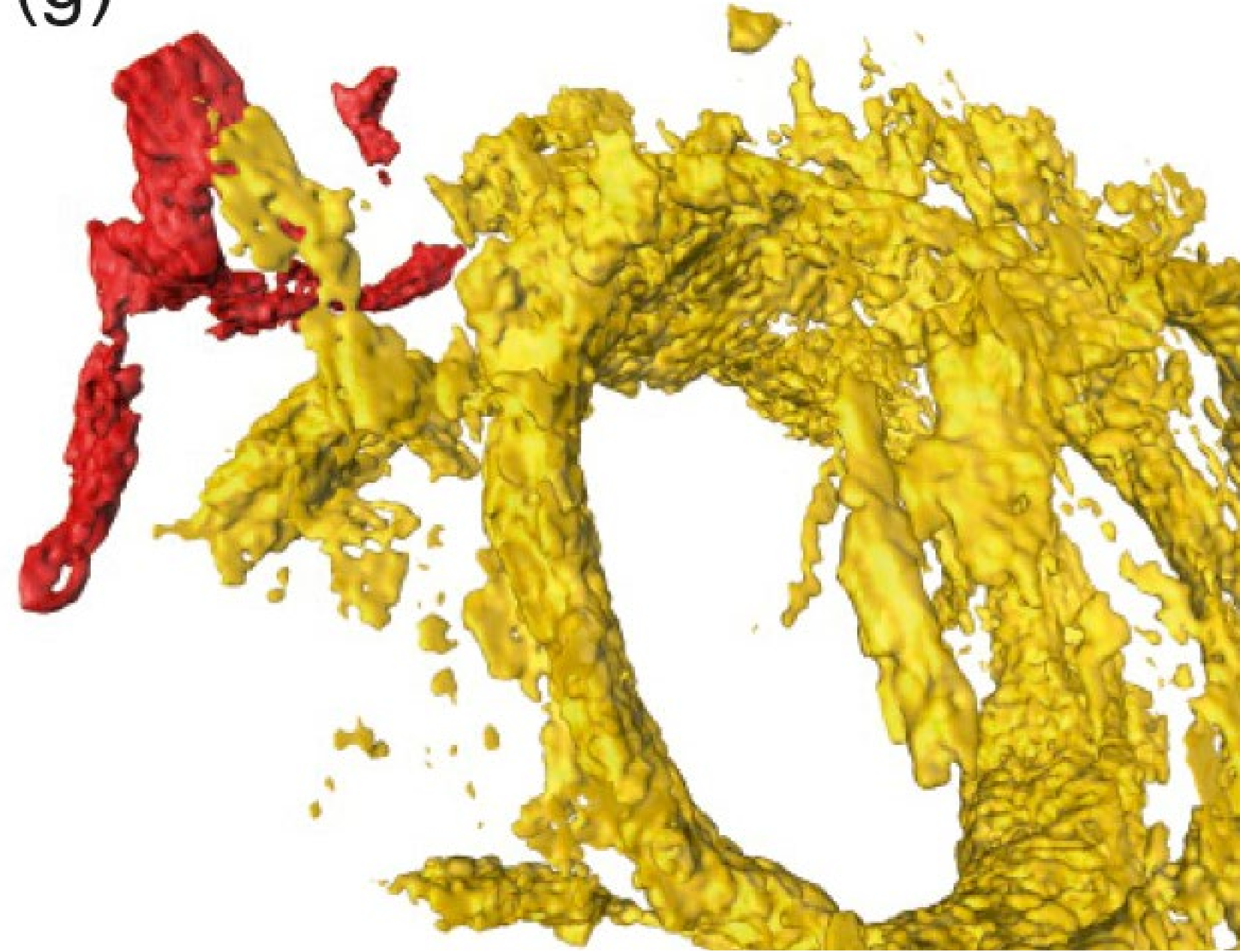


Marius Reichardt et al.:
3D virtual histopathology of cardiac tissue from Covid-19 patients on phase-contrast X-ray tomography, eLife 2021.

(f)

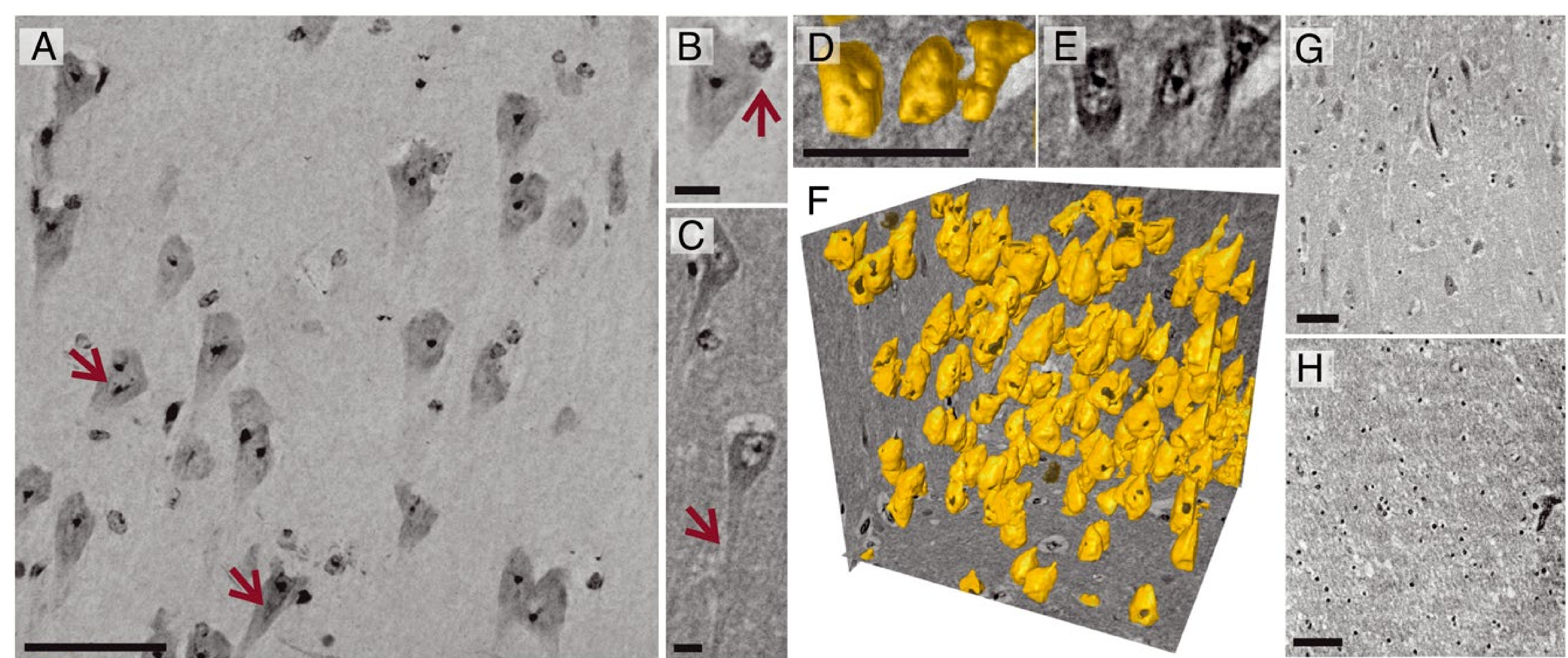


(g)



Marina Eckermann et al.:

3D virtual pathohistology of lung tissue from Covid-19 patients based on phase contrast X-ray tomography, eLife 2020.



M. Eckermann et al.:

3D virtual histology of the human hippocampus based on phase-contrast computed tomography, PNAS 2113835118, 2021

The Golden Age

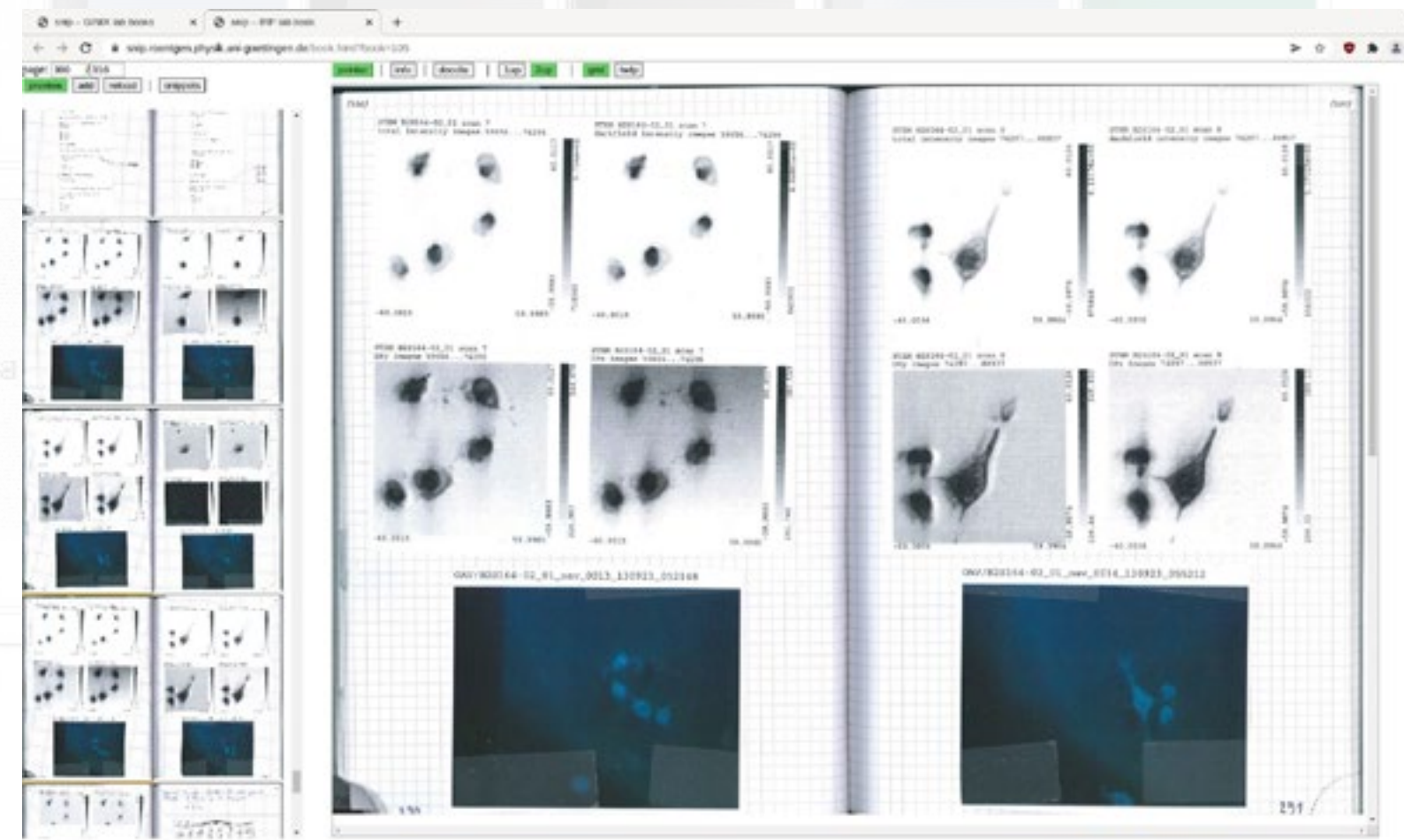
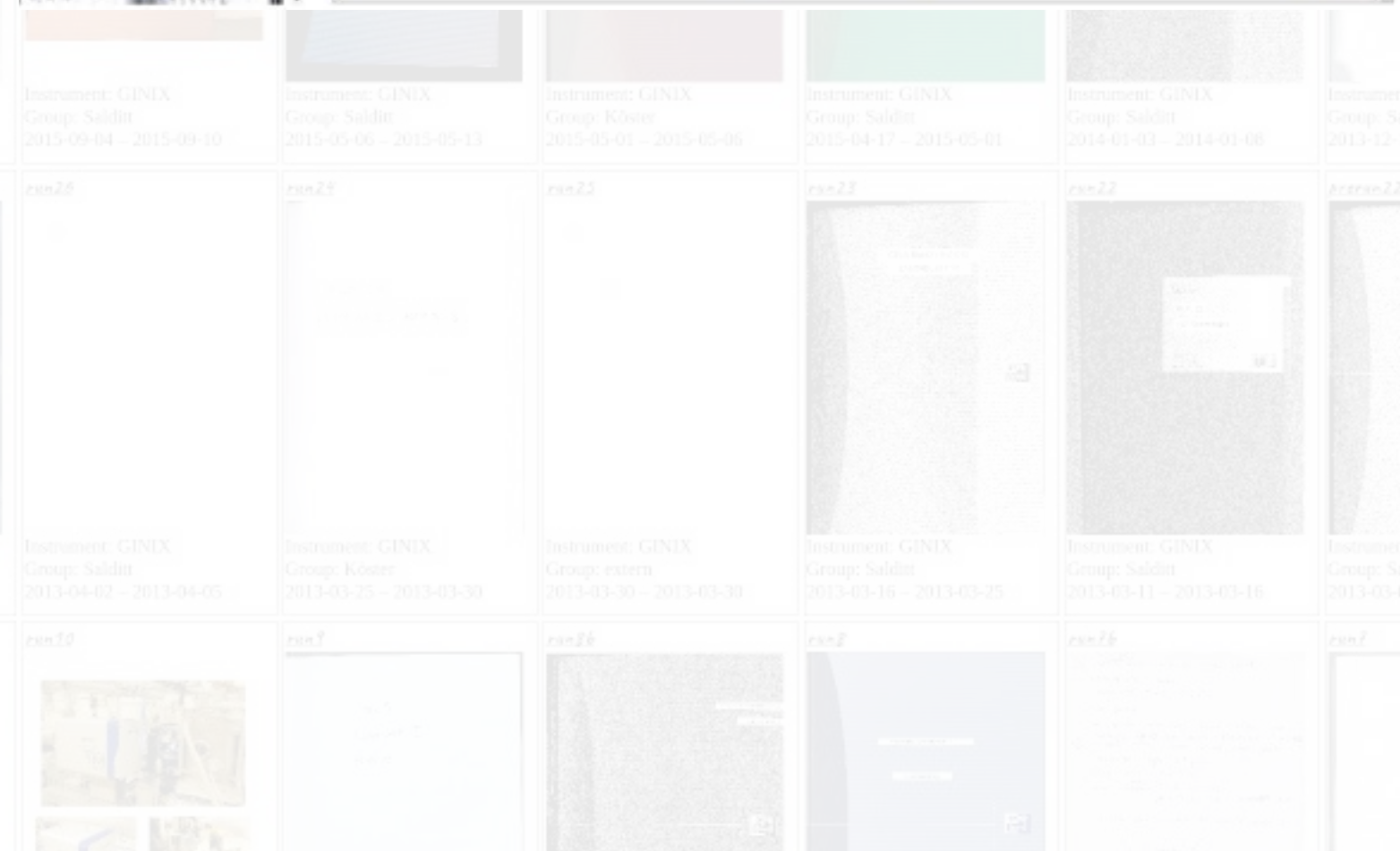
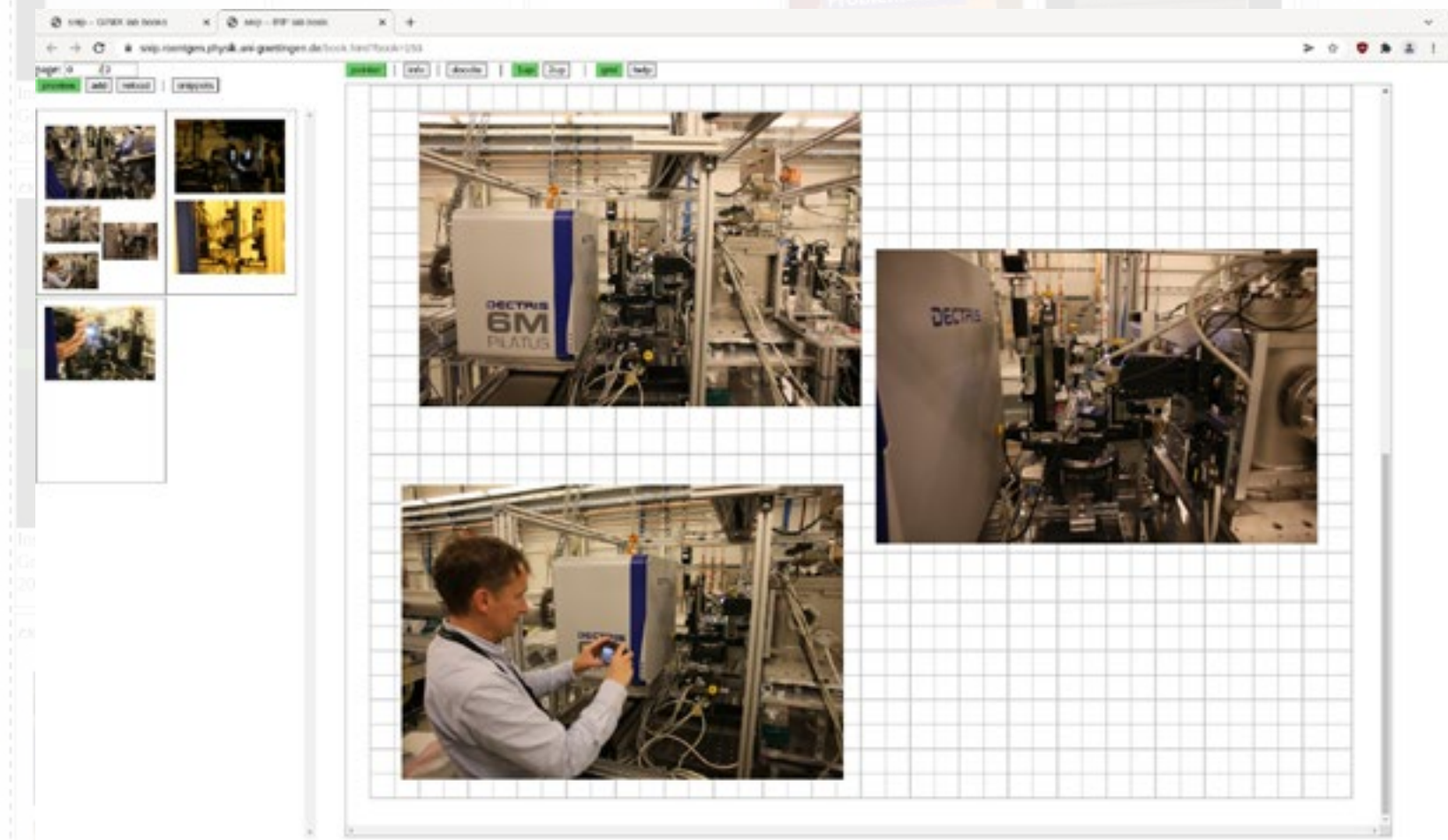
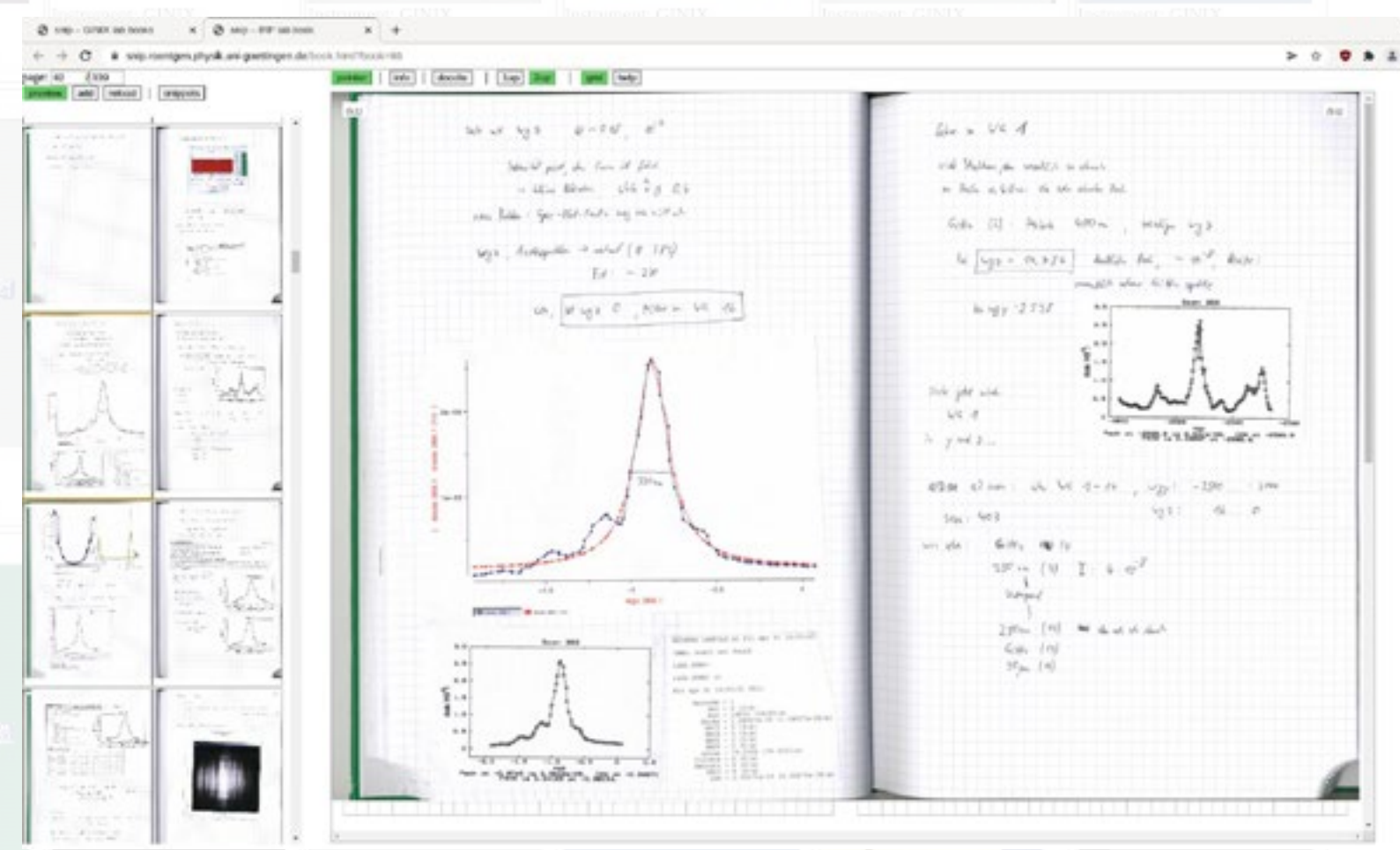
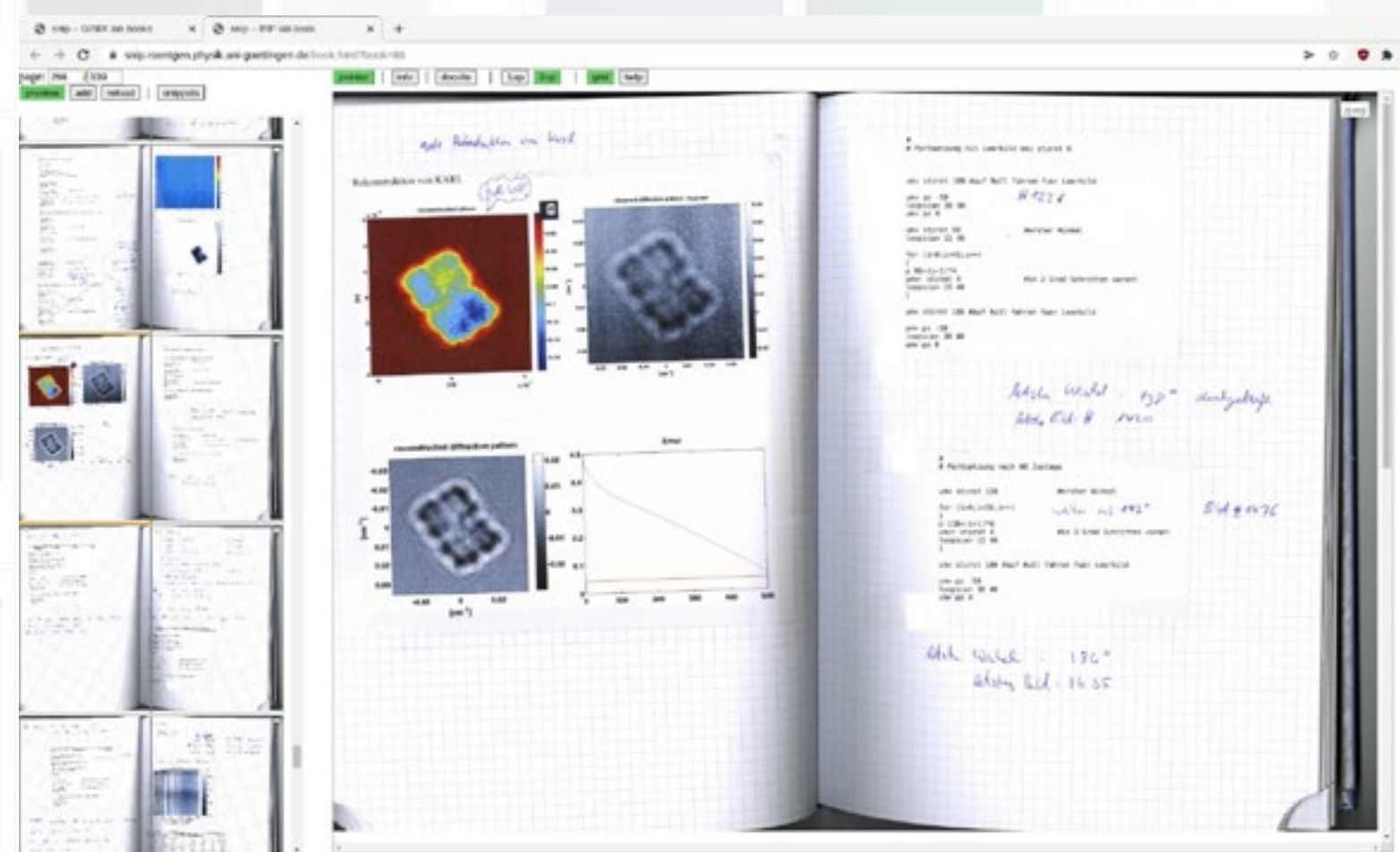
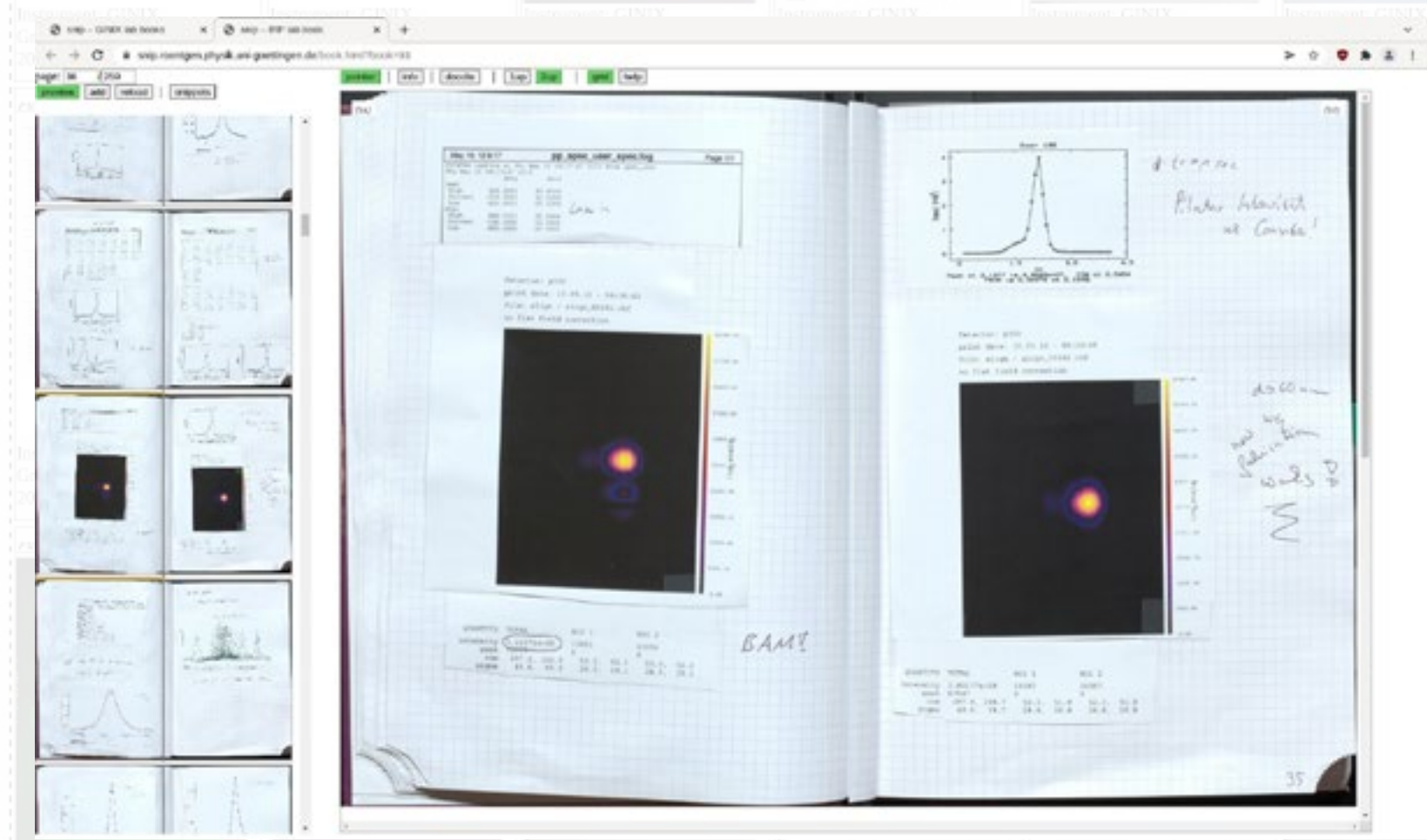
run 9:
Live viewer

run 6:
< 300nm focus

run 6: Karl,
the radiodurans

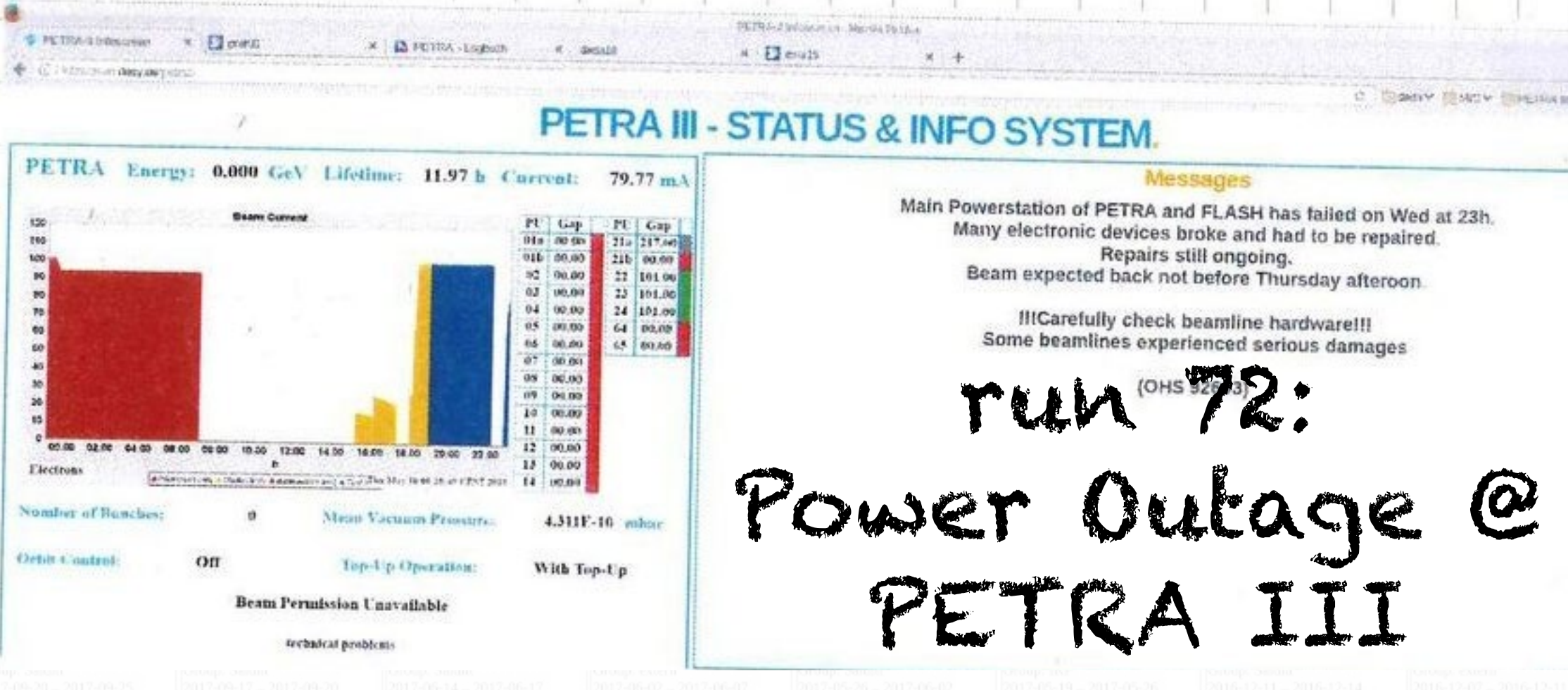
run 33:
Live STXM analysis

run 15: Pilatus 6M
borrowed from P11



STROMAUSFALL: 09 Mai, gegen 23:10
Neustart: 10. Mai, 00:49

Expulsion from Paradise



run 72:
Power Outage @
PETRA III

run 64: Enters Eiger -
with Big Data comes Big Problems

run 74:
beam damage meets big data

Arcadia

run 87:
characterising stzrot

run 100:
FPGA based cont tomo;
digital lab book,
integrated into control software

The screenshot displays a multi-panel interface. The top panel contains handwritten notes in German, including 'Geneticke de SFR 400er in Individualität Selbst' and 'Mög. von Ableitungen/Profilen, in Schritt'. Below the notes are several plots: a waveform plot, a linear plot with a slope, and a histogram. The bottom panel shows four plots of 'mean_positrons_velocity' vs 'Zeit in Sekunden', each with a fitted curve. A handwritten note at the bottom right says 'Zwei Schritte in Phase mit Bremsphase!'.

This screenshot shows a different view of the Arcadia software. A large terminal window in the center displays a shell prompt and a series of commands:

```
1444 SPECF - dosyrun  
Currently all data is stored in /home/desy/20210314  
Do you want to create a new run? (NO)? yes  
please enter name of new run.  
run100  
please enter start date of your beamtime (yyyymmdd) (20210407)? 20210407  
now data will be stored in /home/desy/20210407
```

 To the right of the terminal is a large photograph of the GINIX beamline, with five people standing behind it. The background of the software interface is a grid of smaller panels, some containing plots and others with text.

Utopia

GINIX II @ PETRA IV

SIP 87

Virtual Patho-Histology at the GINIX 3D X-ray Microscope

Markus Osterhoff
Institut für Röntgenphysik,
Uni Göttingen

Introduction

GINIX setup

Holo-Tomo

Methods & Algorithms & AI

Technical Progress, Scientific Results

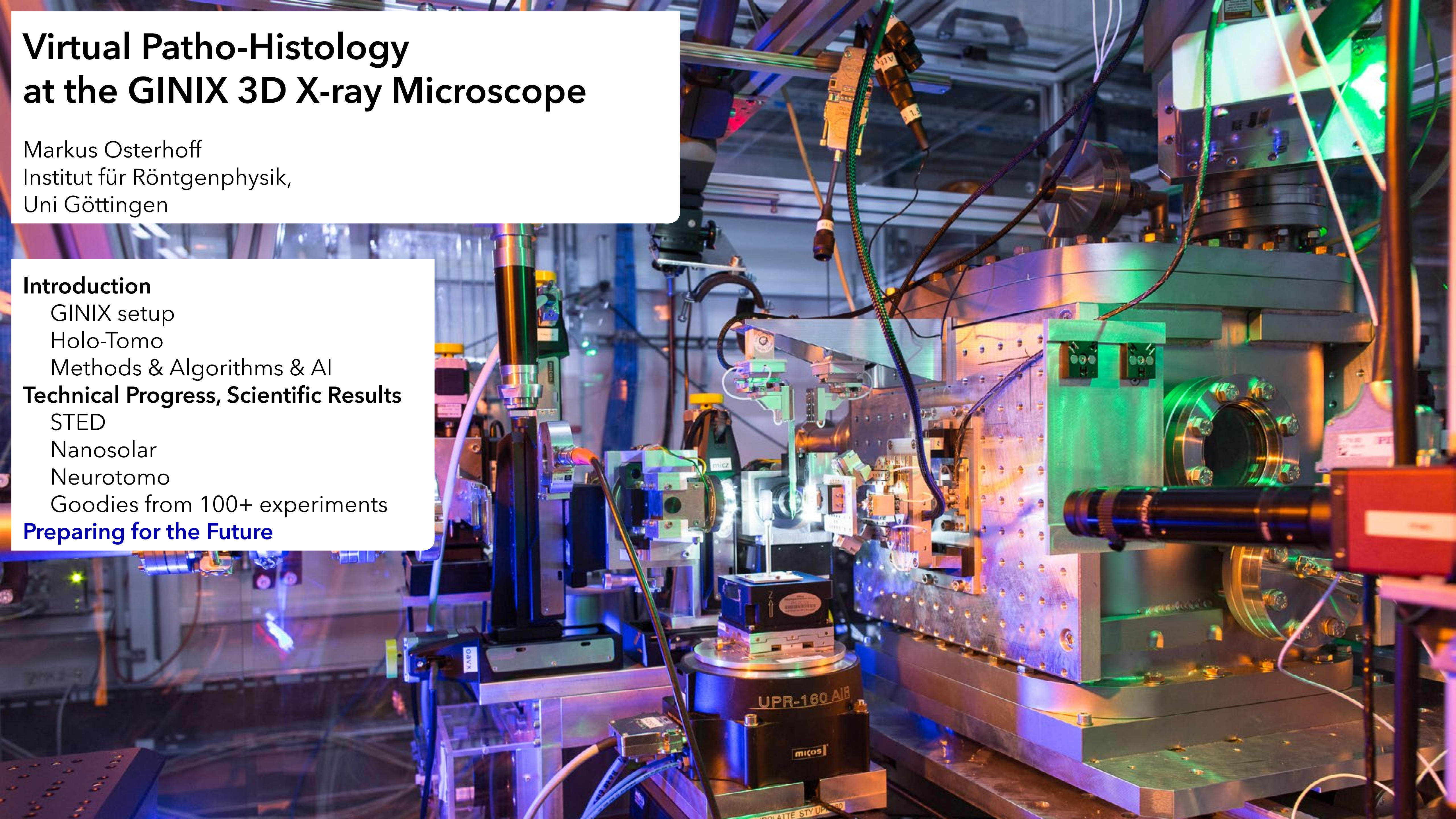
STED

Nanosolar

Neurotomo

Goodies from 100+ experiments

Preparing for the Future



Preparing for the Future

SIP Proposal 87

Holo-Tomography of Biological Tissue beyond the Current Limits

- ▶ Multi-Scale and high resolution
voxel sizes ~ 5 nm - 2 μm
field of view ~ 10 μm - 5 mm
- ▶ Compatibility with physiologic samples environments
in-air, hydrated tissue; robotic sample exchange

PETRA IV Scientific Instrumentation Proposal Holo-Tomography of Biological Tissues beyond the Current Limits

I. Science Case

The unique potential of x-ray holo-tomography for high resolution three-dimensional (3d) analysis of biological samples is by now widely acknowledged [1-17]. This includes studies of biological cells in complex environments, small model organisms, tissues of animal models (diseases/control), and finally human biopsies and autopsies. Notably, 3d virtual histology has emerged as a powerful extension of classical histology, which for the last 100 years has been based on thin sections and light microscopy. 3d histology based on holo-tomography offers full 3d digitalization at an (isotropic) resolution better than with visible light, for large volumes, and without destructive slicing of the tissue. With a dedicated holo-tomography instrument, 3d virtual histology and histo-pathology could be exploited as a new tool for biomedical research, and possibly also for clinical diagnosis based on surgical biopsy punches. This will require a high degree of automation in all workflows from sample shipping, robotic handling, alignment, data recording, reconstruction to segmentation and classification based on artificial intelligence (AI). Such a project would greatly benefit research on cardiovascular, neurodegenerative, and infectious diseases (see Fig.1), and may enable to meet otherwise unsolvable fundamental challenges, such as the unraveling of the connectome in model animals and even the human brain, i.e. the mapping of neuronal circuits in special brain regions. A dedicated instrument could fully unlock the potential of holo-tomography by overcoming the persistent resolution and contrast limits of biological matter encountered today.

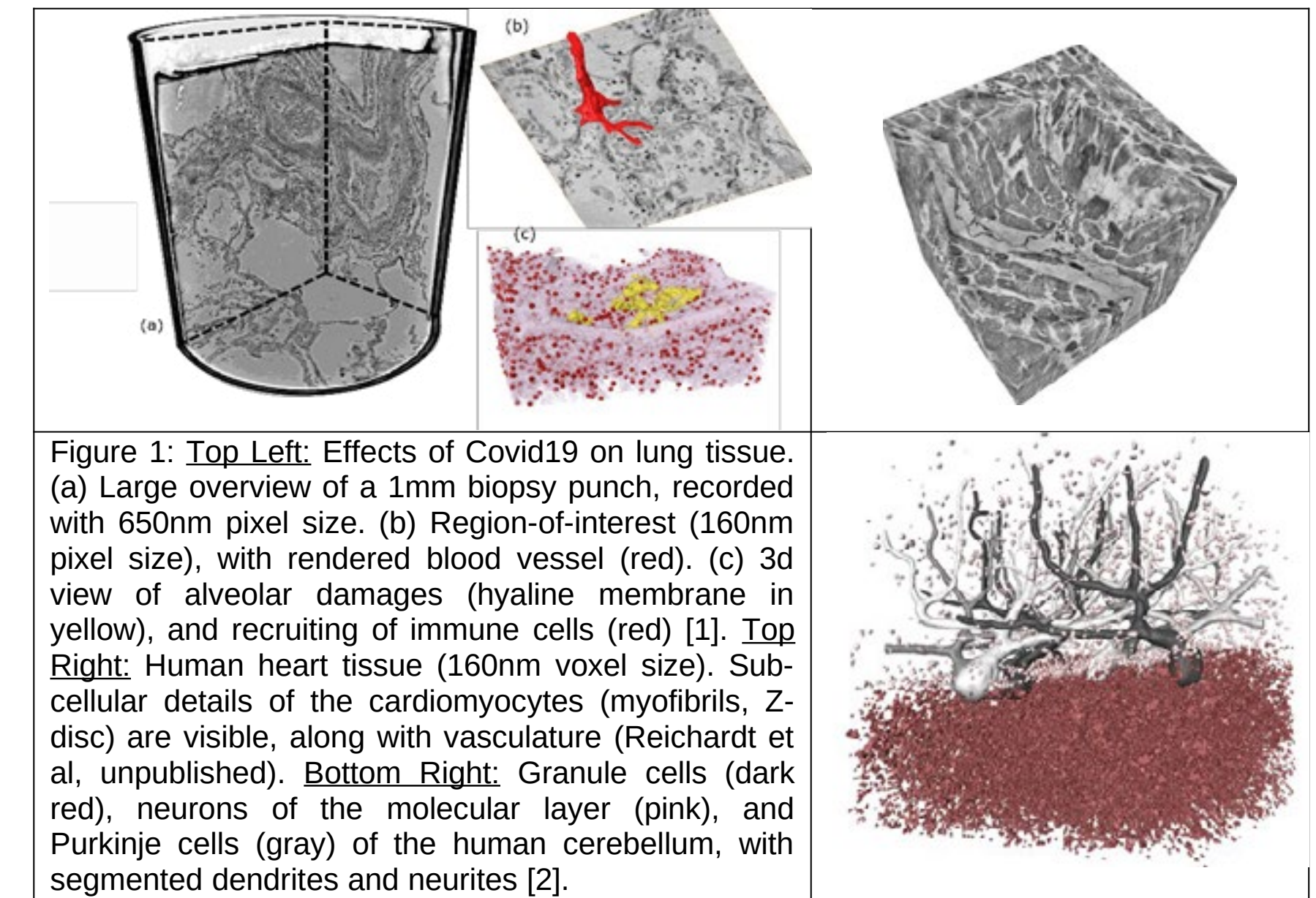


Figure 1: Top Left: Effects of Covid19 on lung tissue. (a) Large overview of a 1mm biopsy punch, recorded with 650nm pixel size. (b) Region-of-interest (160nm pixel size), with rendered blood vessel (red). (c) 3d view of alveolar damages (hyaline membrane in yellow), and recruiting of immune cells (red) [1]. Top Right: Human heart tissue (160nm voxel size). Sub-cellular details of the cardiomyocytes (myofibrils, Z-disc) are visible, along with vasculature (Reichardt et al, unpublished). Bottom Right: Granule cells (dark red), neurons of the molecular layer (pink), and Purkinje cells (gray) of the human cerebellum, with segmented dendrites and neurites [2].

In many applications, the 3d structure has to be studied over multiple length scales. Taking human brain mapping as a highlight example, the instrument should at the same time be able to cover the neuronal cyto-architecture of a biopsy with a field of view of several mm's probed in parallel beam geometry, as well as zooms into regions of interest, with a resolution high enough to identify individual synapses. By achieving a resolution and image quality high enough to reconstruct neuronal circuits, holo-tomography would become an enabling tool for neuroscience. In principle, the projected brilliance of PETRA IV meets these requirements. However, a fully dedicated instrument for holo-tomography with advanced X-ray optics and detection, as well as optimized phase retrieval, reconstruction, and data handling strategies is equally important.

Preparing for the Future

SIP Proposal 87

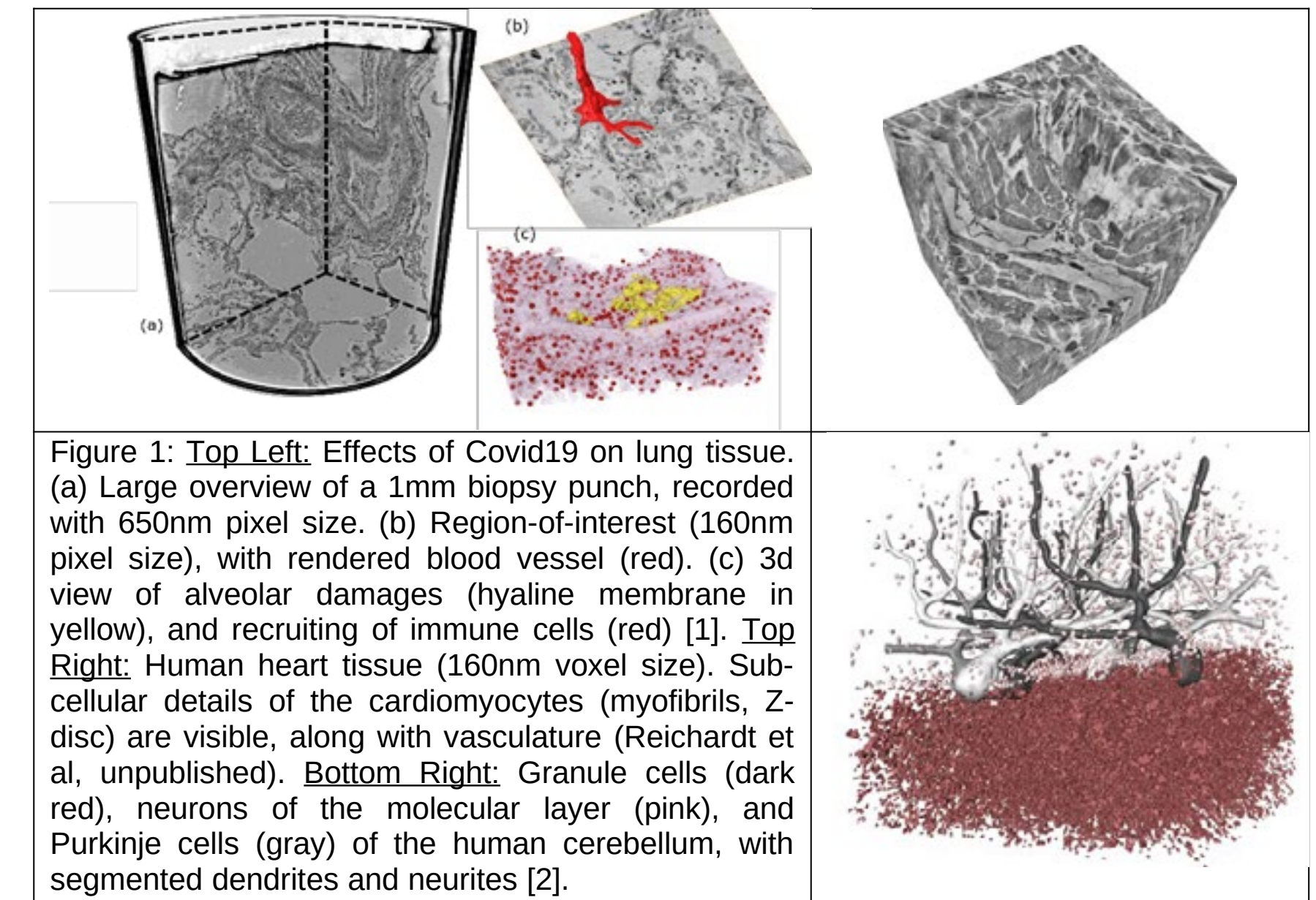
Holo-Tomography of Biological Tissue beyond the Current Limits

- ▶ Multi-Scale and high resolution
voxel sizes $\sim 5\text{ nm} - 2\text{ }\mu\text{m}$
field of view $\sim 10\text{ }\mu\text{m} - 5\text{ mm}$
- ▶ Compatibility with physiologic samples environments
in-air, hydrated tissue; robotic sample exchange
- ▶ Energy range optimised for phase contrast
7 - 16 keV for unstained tissue
21 - 25 keV for larger biological specimens / material science
- ▶ Dose efficiency, high image quality
waveguide-filtered illumination, hybrid pixelated detectors (\sim Eiger 16M)

PETRA IV Scientific Instrumentation Proposal Holo-Tomography of Biological Tissues beyond the Current Limits

I. Science Case

The unique potential of x-ray holo-tomography for high resolution three-dimensional (3d) analysis of biological samples is by now widely acknowledged [1-17]. This includes studies of biological cells in complex environments, small model organisms, tissues of animal models (diseases/control), and finally human biopsies and autopsies. Notably, 3d virtual histology has emerged as a powerful extension of classical histology, which for the last 100 years has been based on thin sections and light microscopy. 3d histology based on holo-tomography offers full 3d digitalization at an (isotropic) resolution better than with visible light, for large volumes, and without destructive slicing of the tissue. With a dedicated holo-tomography instrument, 3d virtual histology and histo-pathology could be exploited as a new tool for biomedical research, and possibly also for clinical diagnosis based on surgical biopsy punches. This will require a high degree of automation in all workflows from sample shipping, robotic handling, alignment, data recording, reconstruction to segmentation and classification based on artificial intelligence (AI). Such a project would greatly benefit research on cardiovascular, neurodegenerative, and infectious diseases (see Fig.1), and may enable to meet otherwise unsolvable fundamental challenges, such as the unraveling of the connectome in model animals and even the human brain, i.e. the mapping of neuronal circuits in special brain regions. A dedicated instrument could fully unlock the potential of holo-tomography by overcoming the persistent resolution and contrast limits of biological matter encountered today.



In many applications, the 3d structure has to be studied over multiple length scales. Taking human brain mapping as a highlight example, the instrument should at the same time be able to cover the neuronal cyto-architecture of a biopsy with a field of view of several mm's probed in parallel beam geometry, as well as zooms into regions of interest, with a resolution high enough to identify individual synapses. By achieving a resolution and image quality high enough to reconstruct neuronal circuits, holo-tomography would become an enabling tool for neuroscience. In principle, the projected brilliance of PETRA IV meets these requirements. However, a fully dedicated instrument for holo-tomography with advanced X-ray optics and detection, as well as optimized phase retrieval, reconstruction, and data handling strategies is equally important.

Preparing for the Future

SIP Proposal 87

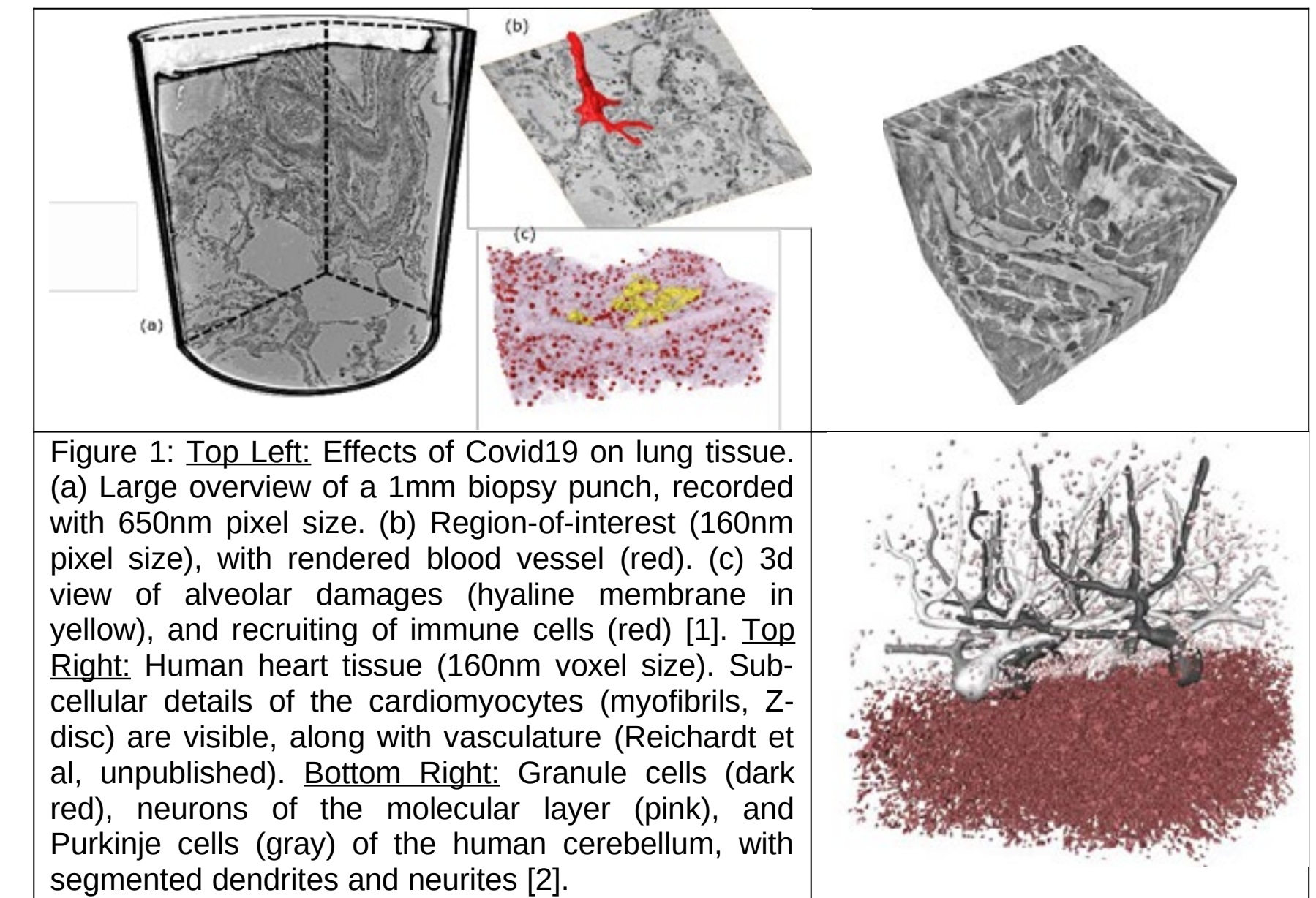
Holo-Tomography of Biological Tissue beyond the Current Limits

- ▶ Multi-Scale and high resolution
voxel sizes $\sim 5\text{ nm} - 2\text{ }\mu\text{m}$
field of view $\sim 10\text{ }\mu\text{m} - 5\text{ mm}$
- ▶ Compatibility with physiologic samples environments
in-air, hydrated tissue; robotic sample exchange
- ▶ Energy range optimised for phase contrast
7 - 16 keV for unstained tissue
21 - 25 keV for larger biological specimens / material science
- ▶ Dose efficiency, high image quality
waveguide-filtered illumination, hybrid pixelated detectors (\sim Eiger 16M)
- ▶ Phase retrieval and Reconstruction
advanced iterative algorithms that overcome empty beam correction
see Jakob Soltau
- ▶ Holistic design of control and data transfer
live real-time reconstruction, standards, auto alignment
processing pipeline from detector data to segmentation data

PETRA IV Scientific Instrumentation Proposal Holo-Tomography of Biological Tissues beyond the Current Limits

I. Science Case

The unique potential of x-ray holo-tomography for high resolution three-dimensional (3d) analysis of biological samples is by now widely acknowledged [1-17]. This includes studies of biological cells in complex environments, small model organisms, tissues of animal models (diseases/control), and finally human biopsies and autopsies. Notably, 3d virtual histology has emerged as a powerful extension of classical histology, which for the last 100 years has been based on thin sections and light microscopy. 3d histology based on holo-tomography offers full 3d digitalization at an (isotropic) resolution better than with visible light, for large volumes, and without destructive slicing of the tissue. With a dedicated holo-tomography instrument, 3d virtual histology and histo-pathology could be exploited as a new tool for biomedical research, and possibly also for clinical diagnosis based on surgical biopsy punches. This will require a high degree of automation in all workflows from sample shipping, robotic handling, alignment, data recording, reconstruction to segmentation and classification based on artificial intelligence (AI). Such a project would greatly benefit research on cardiovascular, neurodegenerative, and infectious diseases (see Fig.1), and may enable to meet otherwise unsolvable fundamental challenges, such as the unraveling of the connectome in model animals and even the human brain, i.e. the mapping of neuronal circuits in special brain regions. A dedicated instrument could fully unlock the potential of holo-tomography by overcoming the persistent resolution and contrast limits of biological matter encountered today.



In many applications, the 3d structure has to be studied over multiple length scales. Taking human brain mapping as a highlight example, the instrument should at the same time be able to cover the neuronal cyto-architecture of a biopsy with a field of view of several mm's probed in parallel beam geometry, as well as zooms into regions of interest, with a resolution high enough to identify individual synapses. By achieving a resolution and image quality high enough to reconstruct neuronal circuits, holo-tomography would become an enabling tool for neuroscience. In principle, the projected brilliance of PETRA IV meets these requirements. However, a fully dedicated instrument for holo-tomography with advanced X-ray optics and detection, as well as optimized phase retrieval, reconstruction, and data handling strategies is equally important.



Figure 3: Schematic view of the envisaged experimental hutch as proposed for the holo-tomography instrument at PETRA IV. A key component is the 25-30m long detector arm required to replace indirect detection in cone-beam holo-tomography by hybrid pixel detectors. This will result in immediate advantages for resolution and dose efficiency. For overview scans with a large field of view, the nano-focus optic is moved and parallel beam scans can be acquired at the same sample position with a microscope-coupled scintillator camera installed on the same goniometer table as the sample tower. Changes of samples are carried out robotically.

Preparing for the Future

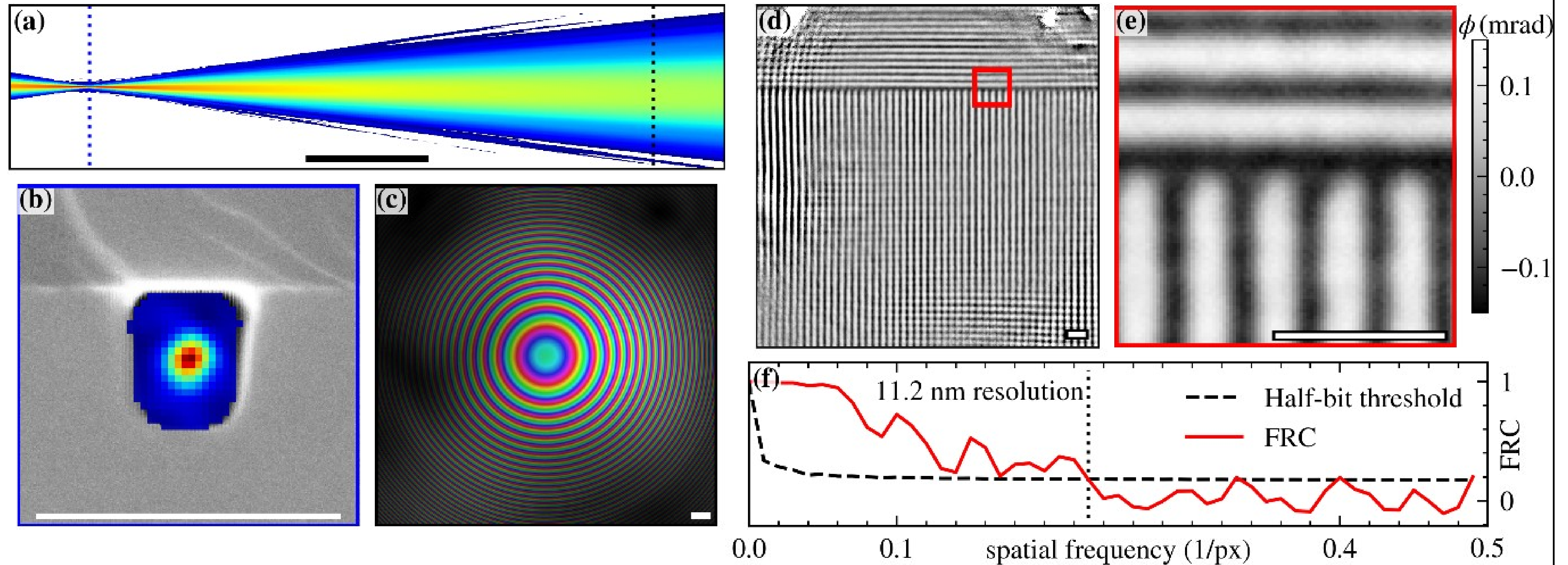


Figure 2: Proof-of-concept of super-resolution holography with pixel detectors: (left) Intensity in waveguide exit plane superimposed with SEM image (100nm scale bar), and phase reconstruction of waveguide illumination in the object plane showing a high-quality spherical phase profile which is used as a constraint in object phase retrieval. (right) Reconstruction of 50nm lines and spaces from a single holographic recording, using a pixel detector (EIGER X4M), and yielding a resolution of 11nm (FSC), roughly a factor of 3 smaller than the waveguide exit spot size (Soltau et al., published! *Optica* 8, 818–823, 2021).

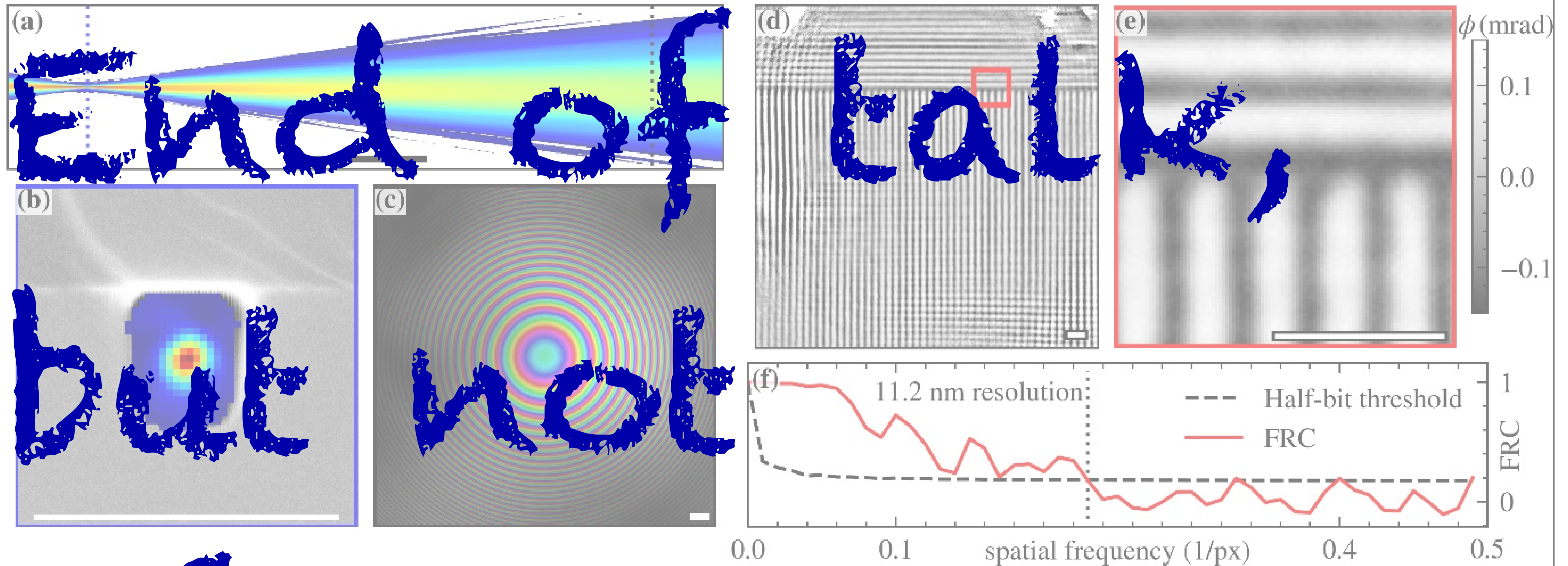


Figure 2: Proof-of-concept of super-resolution holography with pixel detectors: (left) Intensity in waveguide exit plane superimposed with SEM image (100nm scale bar), and phase reconstruction of waveguide illumination in the object plane showing a high quality spherical phase profile which is used as a constraint in object phase retrieval. (right) Reconstruction of 50nm lines and spaces from a single holographic recording, using a pixel detector (EIGER X4M), and yielding a resolution of 11nm (FSC), roughly a factor of 5 smaller than the waveguide exit spot size (Soltau et al., published! Optica 8, 818-823, 2021).